JSHC
Japan Society of Histochemistry and Cytochemistry
Established 1959

Acta Histochem. Cytochem. 45 (2): 83–106, 2012
doi:10.1267/ahc.11034

Review

Development of Ultra-Super Sensitive Immunohistochemistry and Its Application to the Etiological Study of Adult T-Cell Leukemia/Lymphoma

Kazuhisa Hasui[1], Jia Wang[1,5], Yuetsu Tanaka[2], Shuji Izumo[3], Yoshito Eizuru[4] and Takami Matsuyama[1]

[1]Division of Immunology, Department of Infection and Immunity, Institute Research Center (Health Research Course), Kagoshima University Graduate School of Medical and Dental Sciences, [2]Department of Immunology, Graduate School of Medicine, University of the Ryukyus, [3]Chronic Viral Diseases Div. of Molecular Pathology, Center for Chronic Viral Diseases (Infection and Immunity), Institute Research Center (Health Research Course), Kagoshima University Graduate School of Medical and Dental Sciences, [4]Chronic Viral Diseases Div. of Persistent & Oncogenic Viruses, Center for Chronic Viral Diseases (Infection and Immunity), Institute Research Center (Health Research Course), Kagoshima University Graduate School of Medical and Dental Sciences and [5]Present address: INAMORI Frontier Research Center, Kyushu University, 744 Motooka, Nishi-ku, Fukuoka 819–0395, Japan

Received July 15, 2011; accepted February 14, 2012; published online April 21, 2012

Antigen retrieval (AR) and ultra-super sensitive immunohistochemistry (ultra-IHC) have been established for application to archival human pathology specimens. The original ultra-IHC was the ImmunoMax method or the catalyzed signal amplification system (ImmunoMax/CSA method), comprising the streptavidin-biotin complex (sABC) method and catalyzed reporter deposition (CARD) reaction with visualization of its deposition. By introducing procedures to diminish non-specific staining in the original ultra-IHC method, we developed the modified ImmunoMax/CSA method with AR heating sections in an AR solution (heating-AR). The heating-AR and modified ImmunoMax/CSA method visualized expression of the predominantly simple present form of HTLV-1 proviral DNA pX region p40Tax protein (Tax) in adult T-cell leukemia/lymphoma (ATLL) cells in archival pathology specimens in approximately 75% of cases. The simple present form of Tax detected exhibited a close relation with ATLL cell proliferation. We also established a new simplified CSA (nsCSA) system by replacing the sABC method with the secondary antibody- and horse radish peroxidase-labeled polymer reagent method, introducing the pretreatments blocking non-specific binding of secondary antibody reagent, and diminishing the diffusion of deposition in the CARD reaction. Combined with AR treating sections with proteinase K solution (enzymatic-AR), the nsCSA system visualized granular immunostaining of the complex present form of Tax in a small number of ATLL cells in most cases, presenting the possibility of etiological pathological diagnosis of ATLL and suggesting that the complex present form of Tax-positive ATLL cells were young cells derived from ATLL stem cells. The heating-AR and ultra-IHC detected physiological expression of the p53 protein and its probable phosphorylation by Tax in peripheral blood mononuclear cells of peripheral blood tissue specimens from HTLV-1 carriers, as well as physiological and pathological expression of the molecules involved with G1 phase progression and G1–S phase transition (E2F-1, E2F-4, DP-1, and cyclin E) in ATLL and peripheral T-cell lymphoma cells. The ultra-IHC with AR is useful for etiological pathological diagnosis of ATLL since HTLV-1 pathogenicity depends on that of Tax, and can be a useful tool for studies translating advanced molecular biology and pathology to human pathology.

Key words: ultra-super sensitive immunohistochemistry, HTLV-1, p53 protein, cell cycle, adult T-cell leukemia/lymphoma (ATLL)

Correspondence to: Dr. Kazuhisa Hasui, Division of Immunology, Department of Infection and Immunity, Institute Research Center (Health Research Course), Kagoshima University Graduate School of Medical and Dental Sciences, Sakuragaoka 8–35–1, Kagoshima 890–8544, Japan. E-mail: anahasui@m3.kufm.kasgoshima-u.ac.jp

I. Introduction

Adult T-cell leukemia/lymphoma (ATLL) is a type of peripheral T-cell leukemia/lymphoma (PTCL) that is caused

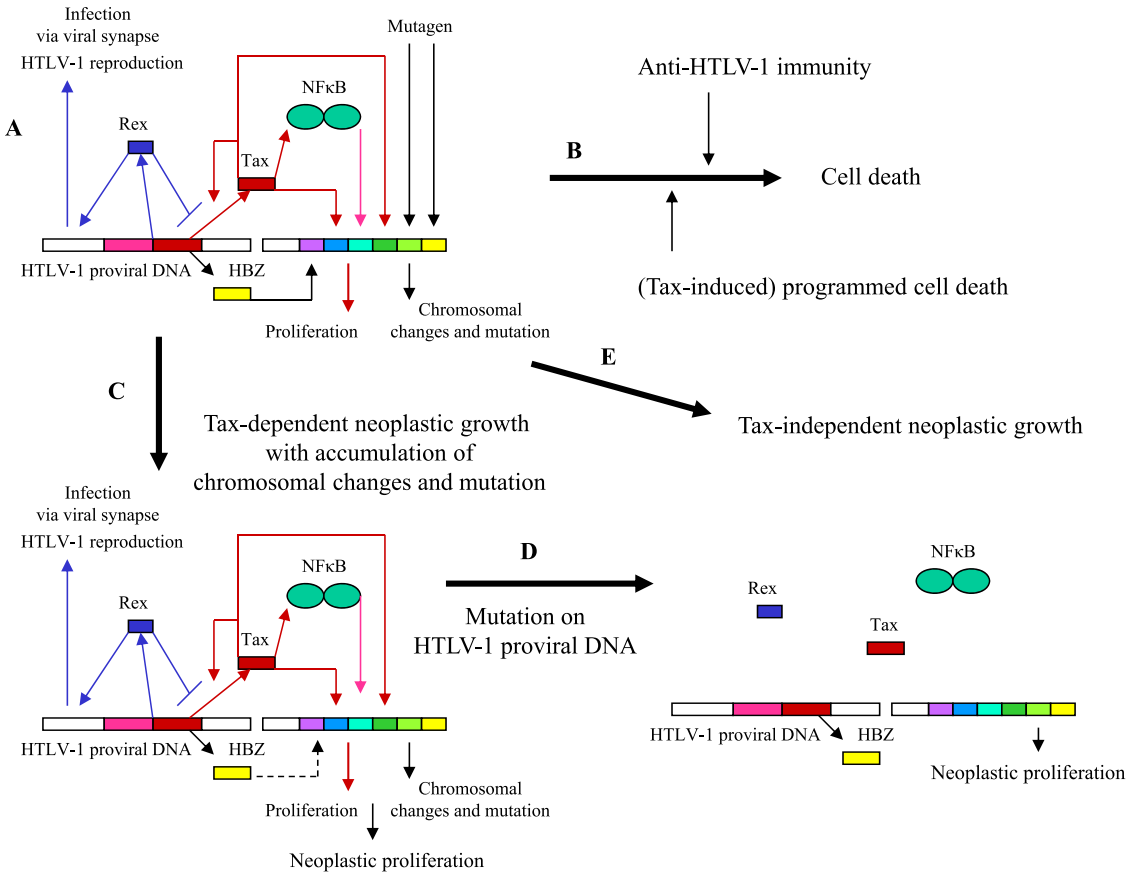

Fig. 1. Pathogenicity of human T-lymphotropic virus type 1 (HTLV-1). ATLL is thought to be caused by pathogenicity of the HTLV-1 proviral DNA pX region p40Tax protein (Tax) and effects of external and internal mutagens. Recently, HTLV-1 basic leucine zipper (HBZ) mRNA from the HTLV-1 proviral DNA minus strand is regarded to cause ATLL independently of Tax. **A**) Latent phase HTLV-1 infection: Tax synthesis is modulated by HTLV-proviral DNA pX region p27Rex protein (Rex). Tax trans-activates and -suppresses host cell genes. HBZ mRNA propels proliferation of the host cells through E2F-1 signaling to the cell cycle. Internal and external mutagens affect host cell genes when APOBEC3G is one of the internal mutagens in activated T-cells. **B**) Anti-HTLV-1 immunity: Anti-HTLV-1 immunity would eliminate HTLV-1 infected T-cells. **C**) Early phase ATLL: Neoplastic proliferation of early ATLL cells depends on Tax in the background of the effects of HBZ mRNA, chromosomal changes and mutations. **D**) Late phase ATLL: Accumulation of chromosomal changes and mutations with and without the effects of Tax, APOBEC3G and the other mutagens confer neoplastic properties to early phase ATLL cells. Tax may disappear and its DNA might be destroyed in most late phase ATLL cells. **E**) Development of a Tax-independent T-cell neoplasm: Depending on the chromosomal changes and mutations induced by the external and internal mutagens and possibly by HBZ mRNA, HTLV-1 infected T-cells may develop into a Tax-independent T-cell neoplasm.

by human T-lymphotropic virus type 1 (HTLV-1) [96]. ATLL occurs in the lifetime of 2 to 5% of HTLV-1 carriers [4]. ATLL is subcategorized clinically into smoldering, including cutaneous type, chronic and acute leukemia, and lymphoma types [89]. Most ATLL patients have anti-HTLV-1 antibodies [36] when ATLL cells exhibit monoclonal integration of HTLV-1 proviral DNA [109, 111].

In the natural history of HTLV-1 infection, following latent infection spanning more than 30 years from the initial infection in the perinatal period (Fig. 1) and based on virological, molecular biological and immunological understanding of HTLV-1 infection, early-phase ATLL cells with neoplastic properties dependent on the HTLV-1 proviral DNA pX region p40Tax protein (Tax) [42, 70, 80, 93, 101, 110] appear under the effects of external and internal mutagens [19, 76, 84] following the accumulation of mutations induced by repeated Tax expression [18] in the background of persistent proliferation of HTLV-1-infected T-cells, which is probably induced by HTLV-1 basic leucine zipper (HBZ) mRNA [64, 65]. Then, late-phase ATLL cells with neoplastic properties independent of Tax appear when mutation has progressed in the host cell DNA and HTLV-1 proviral DNA including pX p40Tax DNA sequence [19].

ATLL cells exhibit the $CD4^+$ $CD25^+$ forkhead box protein $P3^+$ ($Foxp3^+$) phenotype of regulatory T-cells [108]. PTCL in a patient with anti-HTLV-1 antibodies or with clinicopathological information of HTLV-1 proviral DNA integration is diagnosed practically as ATLL. On the other hand, etiological pathological diagnosis of ATLL is expected based on immunohistochemistry (IHC) detecting of

A. Super sensitive IHC (ordinary-IHC) methods related to ultra-IHC

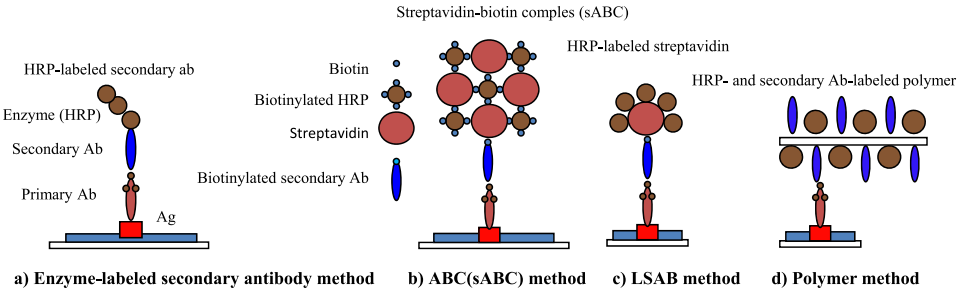

a) Enzyme-labeled secondary antibody method **b) ABC(sABC) method** **c) LSAB method** **d) Polymer method**

B. Ultra-IHC by means of CARD reaction

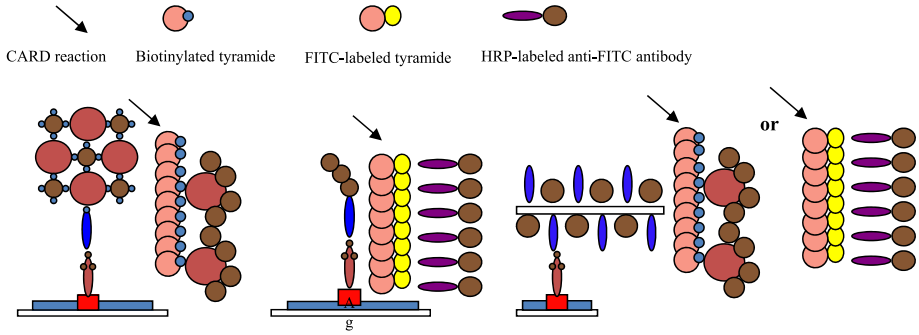

e) ImmunoMax/CSA method **f) Dako CSA II system** **g) New simplified CSA system**

C. Pretreatments for ultra-IHC by means of CARD reaction

	Pretreatment				
	Inactivation of endogenous peroxidase	Suppression of non-specific staining of primary antibody	Masking of endogenous biotin	Suppression of non-specific staining of secondary antibody	Suppression of non-specific staining in CARD reaction
Original ImmunoMax/CSA method	○	○	-	-	-
Modified ImmunoMax/CSA method	○ **(2 times)**	○	○	-	-
Dako CSA II system	○	○	-	-	-
New simplified CSA system	○ **(2 times)**	○	-	○	○

Fig. 2. Products of super and ultra-super sensitive immunohistochemistry (IHC) and pretreatments for ultra-super sensitive IHC (ultra-IHC). Differences among enzyme-labeled antibody indirect methods can be observed in their products and in each method's pretreatments. **A**) Super sensitive IHC (ordinary-IHC) methods related to ultra-IHC are **a**) classic enzyme-labeled secondary antibody method, **b**) avidin (streptavidin)-biotin complex method (ABC/sABC method), **c**) horse radish peroxidase (HRP)-labeled streptavidin-biotin complex method (LSAB method, and **d**) HRP- and secondary antibody-labeled polymer reagent method (Polymer method). **B**) Ultra-IHC by means of catalyzed reporter deposition (CARD) reaction. The original ImmunoMax/CSA method (**e**) comprises the sABC method (**b**) and a CARD reaction with detection of deposited biotinylated tyramide by the LSAB method (**c**). Dako CSA II system (**f**), a biotin-free system, comprises the enzyme-labeled secondary antibody method (**a**) and CARD reaction with detection of deposited FITC-labeled tyramide with HRP-labeled anti-FITC antibody. The new simplified CSA system (**g**) comprises the polymer method and CARD reaction with detection of deposited biotinylated tyramide by the LSAB method (**c**) or with detection of deposited FITC-labeled tyramide with HRP-labeled anti-FITC antibody. **C**) Pretreatment for ultra-IHC with the CARD reaction. The original ImmunoMax/CSA method is equipped with pretreatments for endogenous peroxidase and non-specific binding of the primary antibody. The modified ImmunoMax/CSA method introduces masking of endogenous biotin in itself. The Dako CSA II system is not equipped with additional pretreatments besides those available in the original ImmunoMax/CSA method. The new simplified CSA system is equipped with additional pretreatments for non-specific binding of the secondary antibody and non-specific staining in CARD reaction.

Tax, HTLV-1 proviral DNA pX p27Rex protein (Rex) and HBZ mRNA/protein in PTCL cells. However, the amount of Tax, Rex and HBZ protein in ATLL cells is too small to be detected by ordinary super sensitive enzyme-labeled antibody methods of IHC (ordinary-IHC) such as avidin/streptavidin-biotin complex (ABC/sABC, Fig. 2b), labeled streptavidin-biotin complex method (LSAB, Fig. 2c), and polymer methods (Fig. 2d). Therefore, these proteins should be detected by ultra-super sensitive IHC (ultra-IHC) comprising an indirect enzyme-labeled antibody method and catalyzed reporter deposition (CARD) reaction (Fig. 2e). Some ultra-IHC kits are commercially available but suffer from strong non-specific staining. We have succeeded in developing ultra-IHC of Tax and Rex on routine paraffin sections of ATLL [30, 31, 35, 62], solving the problems that cause the strong non-specific staining.

This review describes our development of the ultra-IHC and its application, which employs anti-HTLV-1-related antibodies, to the pathological diagnosis of ATLL and the analysis of ATLL oncogenesis and pathogenesis.

II. Development of Ultra-IHC

Antigen retrieval (AR) heating sections in an AR solution such as 0.01 M citrate buffer, pH 6.0 (heating-AR) heralded the era of so-called paraffin section IHC in the 1990s [86–88]. Currently, many antigens can be detected in archival human pathology specimens by combining heating-AR with ordinary-IHC. In ultra-IHC, heating-AR retrieves larger amounts of antigen based on autoclaving (121°C for 5 min), pressure cooking (for 10 min after boiling) and microwaving (3 times heating for 1 min) but also yields more non-specific staining, whereas heating-AR in 4 M urea solution demonstrated less non-specific staining than heating in 0.01 M citrate buffer [27, 30]. Since the J chain in immunoglobulins A and M and amyloid protein are unmasked by rinsing sections in a solution of highly concentrated denaturing reagent such as urea at 4°C overnight [17, 71], the heating-AR in 4 M urea is also expected to denature and expose antigens to the antibody. Recently, heating-AR has often been performed independently of the AR solution pH [104]. On the other hand, AR treating sections with an enzyme such as proteinase K (enzymatic-AR) is expected to enable visualization of molecules that form complexes or bind with other proteins and DNA, etc. by partly digesting the molecule/tissue complexes obscuring the target molecules [50].

Ultra-IHC was introduced in the field of surgical pathology as the original ImmunoMax/CSA method [67] (Fig. 2e), comprising heating-AR, sABC method (Fig. 2b), CARD reaction (Fig. 2B) and detection of the CARD deposition by LSAB method (Fig. 2c). The ImmunoMax method employed serum solutions such as phosphate buffer saline (PBS) containing 8% horse serum or 8% human AB type serum for blocking non-specific binding (Protein block) of the primary antibody, while CSA system used a serum-free solution such as PBS containing 0.25% casein

Table 1. *Protocols of ultra-super sensitive immunohistochemistry*

A) Protocol of modified ImmunoMax/Catalyzed signal amplification (CSA) method

Step	Work
a	Deparaffinization.
b	First inactivation of endogenous peroxidase (IEP) rinsing sections in methanol containing 0.3% H_2O_2 for 20 min.
c	Antigen retrieval
d	Rinse sections in phosphate buffer saline (PBS).
	Set slides to the autostainer.
1	Second IEP rinsing sections in PBS containing 3% H_2O_2 for 5 min.
2–4	3 times Rinse1
5	*Protein block suppressing non-specific binding of primary antibody for 5 min.
6	**Primary antibody reaction** for 15 min.
7–9	3 times Rinse1
10	Endogenous biotin mask (1) rinsing in avidin solution for 15 min.
11–13	3 times Rinse1
14	Endogenous biotin mask (2) rinsing in biotin solution for 15 min.
15–17	3 times Rinse1
18	**Protein block suppressing non-specific binding of secondary antibody for 5 min.
19	**Biotinylated secondary antibody reaction** for 15 min.
20–22	3 times Rinse1
23	**Horse radish peroxidase (HRP)-labeled streptavidin reaction** for 15 min.
24–26	3 times Rinse1
27	***Protein block suppressing diffusion of catalyzed tyramide in the Catalyzed reporter deposition (CARD) reaction for 1 min.
28	**CARD reaction** for 15 min.
29–30	2 times Rinse2
31	**HRP-labeled streptavidin reaction** for 15 min
32–33	2 times Rinse2
34	**H_2O_2-Diaminobenzidine (DAB) reaction** for 5 min.
35	Rinse with distilled water to stop the DAB reaction.
36	Counterstaining of nuclei
37	Rinse with distilled water.
	Remove slides from the autostainer.
	Dehydrate slides and mount section with plastic medium.

Rinse1: Rinse with Tris buffer saline containing 0.1% Tween 20 (TBST) warmed at 35°C.

Rinse2: Rinse with TBST warmed at 35°C. But the rinsing buffer is PBS at room temperature in a case when a rinsing buffer can be changed by a semi-autostainer (MicroProbe™, Fisher Scientific Co.).

*: Protein block employs PBS containing 0.25% casein (Dako) with 8% horse serum.

**: Protein block employs PBS containing 0.25% casein (Dako) with 8% goat serum.

***: Protein block employs PBS containing 0.25% casein (Dako) or PBS with 3% BSA.

Steps 18 and 27 were inserted according to the new simplified CSA system (Table 1C).

Table 1. Continued (1).

B) The protocol of Dako CSA II system, modified according to new simplified CSA system

Step	Work
a	Deparaffinization.
b	Antigen retrieval
c	Rinse sections in PBS

Set slides to the autostainer.

1	inactivation of endogenous peroxidase rinsing sections in methanol containing 0.3% H_2O_2 for 20 min.
2–4	3 times Rinse1
5	*Protein block for 5 min.
6	**Primary antibody reaction** for 15 min.
7–9	3 times Rinse1
10	**Protein block for 5 min.
11	**HRP-labeled secondary antibody reaction** for 15 min.
12–14	3 times Rinse1
15	***Protein block for 1 to 5 min.
16	**CARD reaction of fluorescein isothiocyanate (FITC)-labeled tyramide** for 30 min.
17–18	2 times Rinse2
19	**HRP-labeled anti-FITC antibody reaction** for 30 min.
20–21	2 times Rinse2
22	**H_2O_2-DAB reaction** for 5 min.
23	Rinse with distilled water to stop the DAB reaction.
24	Counterstaining of nuclei
25	Rinse with distilled water.

Remove slides from the autostainer.

Dehydrate slides and mount section with plastic medium.

Steps 10 and 15 are inserted according to the new simplified CSA system (Table 1C).
Rinse1: Rinse with Tris buffer saline containing 0.1% Tween 20 (TBST) warmed at 35°C.
Rinse2: Rinse with TBST warmed at 35°C. But the rinsing buffer is PBS at room temperature in a case when a rinsing buffer can be changed by a semi-autostainer (MicroProbe™, Fisher Scientific Co.).
Rinse: Post-reaction wash with TBST at room temperature.
*: Protein block employs PBS containing 0.25% casein (Dako) with 8% horse serum.
**: Protein block employs PBS containing 0.25% casein (Dako) with 8% goat serum.
***: Protein block suppresses diffusion of depositing FITC-labeled tyramide in the CARD reaction, pre-treating sections with PBS containing 3% polyethylene glycol (PEG) #20000 and 0.1% Tween 20 or with PBS containing 0.3% BSA and 0.1% Tween 20.

for Protein block. As molecular biology developed, the amounts of molecules traditionally targeted by IHC, such as those of signal transduction molecules and phosphorylated functional proteins, became too minute to be visualized by ordinary-IHC. Then, the ultra-IHC was expected to detect much smaller amounts of molecules, amplifying the ordinary-IHC signals a thousand times through the CARD reaction.

Unfortunately, the original ImmunoMax/CSA method required 2 times horse-radish peroxidase (HRP) reaction in

Table 1. Continued (2).

C) New simplified CSA system (nsCSA system)

Step	Work
a	Deparaffinization.
b	First inactivation of endogenous peroxidase (IEP) rinsing sections in methanol containing 0.3% H_2O_2 for 20 min.
c	Antigen retrieval
d	Rinse sections in PBS

Set slides to the autostainer.

1	Second IEP rinsing sections in PBS containing 3% H_2O_2 for 5 min.
2–4	3 times Rinse1
5	*Protein block for 5 min.
6	**Primary antibody reaction** for 15 min.
7–9	3 times Rinse1
10	**Protein block for 5 min.
11	**HRP- and secondary antibody-labeled polymer reagent reaction** for 15 min.
12–14	3 times Rinse1 (Go to step15)
15	***Protein block for 1 min.
16	**CARD reaction of biotinylated tyramide** for 15 min.
17–18	2 times Rinse2
19	**HRP-labeled streptavidin reaction** for 15 min.
20–21	2 times Rinse2 (Go to step 22)

In a case employing FITC-labeled tyramide.

15	****Protein block for 1 min.
16	**CARD reaction of FITC-labeled tyramide** for 30 min.
17–18	2 times Rinse2
19	**HRP-labeled anti-FITC antibody reaction** for 30 min.
20–21	2 times Rinse2 (Go to step 22)

22	**H_2O_2-DAB reaction** for 5 min.
23	Rinse with distilled water to stop the DAB reaction.
24	Counterstaining of nuclei
25	Rinse with distilled water.

Remove slides from the autostainer.

Dehydrate slide and mount section with plastic medium.

Rinse1: Rinse with Tris buffer saline containing 0.1% Tween 20 (TBST) warmed at 35°C.
Rinse2: Rinse with TBST warmed at 35°C. But the rinsing buffer is PBS at room temperature in a case when a rinsing buffer can be changed by a semi-autostainer (MicroProbe™, Fisher Scientific Co.).
*Protein block: Protein block suppresses non-specific binding of primary antibody, rinsing sections in PBS containing 0.25% casein (Dako) with 8% horse serum or in PBS containing 3% BSA and 8% horse or goat serum
**Protein block: Protein block suppresses non-specific binding of secondary antibody, rinsing sections in PBS containing 0.25% casein (Dako) with 8% goat serum or in PBS containing 3% BSA and 8% goat serum.
***Protein block: Protein block suppresses diffusion of depositing biotinylated tyramide in the CARD reaction, pre-treating sections with PBS containing 0.25% casein (Dako) or PBS with 3% BSA.
****Protein block: Protein block suppresses diffusion of depositing FITC-labeled tyramide in the CARD reaction, pre-treating sections with PBS containing 3% polyethylene glycol (PEG) #20000 and 0.1% Tween 20 or with PBS containing 0.3% BSA and 0.1% Tween 20.

the CARD reaction and diaminobenzidine (DAB)-H_2O_2 reaction for visualization and 2 times biotin-streptavidin binding reaction in the sABC method and in the LSAB method detecting deposited catalyzed tyramide. Moreover, its post-reaction wash appeared incomplete. Therefore, the original ImmunoMax/CSA method (Fig. 2C, Original ImmunoMax/CSA method) amplified an extremely low level of residual activity of endogenous peroxidase, a rather small amount of endogenous biotin, and a trace level of residual reaction reagents into a huge amount of non-specific staining. Thus, the modified ImmunoMax/CSA method (Table 1A) was designed [30] to diminish non-specific staining by introducing double inactivation of endogenous peroxidase before and after AR, endogenous biotin mask treating sections with avidin and biotin solutions between the primary antibody and biotinylated secondary antibody reactions (Fig. 2C, Modified ImmunoMax/CSA method), and the post-reaction wash (PR wash) 3 times in Tris-buffered saline containing 0.5% Tween 20 (TBST) warmed to 35°C [30]. The modified ImmunoMax/CSA method employed PBS containing 8% horse serum and 0.25% casein for Protein block before the primary antibody reaction. Biotinylated tyramide deposited in the CARD reaction was washed out by rinsing 3 times in the warmed TBST so the PR wash following the CARD reaction was defined as rinse twice in PBS at room temperature when the PR wash solution could be changed [30]. Finally, the modified ImmunoMax/CSA method comprised 37 steps in an autostainer (Table 1A), where 2 steps of Protein block for the secondary antibody reaction (step 18, Table 1A) and pretreatment for the reaction (step 27, Table 1A) were those employed in the new simplified CSA (nsCSA) system (Table 1C).

However, non-specific staining persisted somewhat in the modified ImmunoMax/CSA method, and varied with each case. The positive staining of the modified ImmunoMax/CSA method was evaluated in comparison with staining performed without the primary antibody reaction (negative control staining). To prevent non-specific staining caused by endogenous biotin, Dako supplied a CSA II system (Table 1B) to replace the sABC method (Fig. 2b) and the biotinylated tyramide-CARD reaction with HRP-labeled secondary antibody method (Fig. 2a) and the fluorescein isothiocyanate (FITC)-labeled tyramide-CARD reaction (Fig. 2f) but did not equip the Protein block to suppress non-specific binding of the secondary antibody and the pretreatment to suppress the diffusion of catalyzed FITC-labeled tyramide (Fig. 2C, Dako CSA II system). Then, non-specific background staining with the Dako CSA II system was quite high. On the other hand, we developed new simplified CSA system (nsCSA system) (Table 1C, Fig. 2g), replacing the sABC method (Fig. 2b) with the HRP- and secondary antibody-labeled polymer reagent method (Fig. 2d), where additional Protein block suppressed non-specific binding of the polymer reagent and pretreatment suppressed diffusion of the catalyzed biotinylated or FITC-labeled tyramide (Fig. 2C, new simplified CSA system) [28, 34].

The reagent for the Protein block was PBS containing 0.25% casein or 3% bovine serum albumin (BSA), diminishing non-specific staining of the primary antibody and polymer reagents in the nsCSA system [28, 34]. It may have been because the blocking reagent can mask most non-specific binding sites, whereas competitive blocking by the blocking reagent in the primary antibody and polymer reagents would mask approximately half of all non-specific binding sites. Catalyzed tyramide rarely diffused to be deposited in areas distant from CARD reaction sites. Pretreatment with biochemically inactive molecules was required to achieve deposition of catalyzed tyramide much nearer to the CARD reaction sites. The pretreatment reagent was PBS containing 0.25% casein or PBS containing 3% BSA and 0.1% Tween 20 for the biotinylated tyramide-CARD reaction, while PBS containing 3% polyethylene glycol (PEG) #20000 and 0.1% Tween 20 or PBS containing 0.3% BSA and 0.1% Tween 20 was employed for the FITC-labeled tyramide-CARD reaction [28]. The nsCSA system of the biotinylated tyramide-CARD reaction was free from non-specific staining of endogenous biotin even in endogenous biotin-rich tissue such as that from the liver [28]. Antigen detection sensitivity was high in the following order: nsCSA system with the biotinylated tyramide-CARD reaction (Table 1C), nsCSA system with the FITC-labeled tyramide-CARD reaction (Table 1C), and the Dako CSA II system (Table 1B) with pretreatments diminishing non-specific staining according to nsCSA system [28] because the polymer reagent method (Fig. 2d) in the nsCSA system was more sensitive than that of the HRP-labeled secondary antibody method (Fig. 2a) in the CSA II system.

Protein block (PBS containing 0.25% casein, Dako) was a powerful reagent in the nsCSA system but the procedure, which exceeded 15 min, prevented antigen-antibody reaction, whereas PBS containing 3% BSA did not [28]. However, ultra-IHC employing PBS containing 3% BSA encountered non-specific staining through the unexpected anti-BSA antibody that had contaminated the secondary antibody reagent. Affinity-purified secondary antibody reagent might be free from such contamination. As mentioned in the following chapter of enzymatic-AR and ultra-IHC of Tax, non-specific staining in B-cell malignant lymphoma cells may be that of a part of an antibody known as the Fc (Fragment, crystallizable) region. This kind of non-specific staining cannot be suppressed by the PBS containing 0.25% casein and the nsCSA system may require additional Protein block with PBS containing 8% horse serum prior to the primary antibody reaction and with PBS containing 8% goat serum prior to the secondary antibody-polymer reagent reaction.

Furthermore, an adequate concentration of CARD reaction-amplification reagent must be determined because the amplification reagent of FITC-labeled tyramide from the CSA II system yielded a larger amount of non-specific staining than that of biotinylated tyramide from the nsCSA system [28].

III. Application of Ultra-IHC of HTLV-1 Tax to Etiological Diagnosis of ATLL and Related Lesions

The pathogenicity of HTLV-1 infection that causes ATLL is thought to be that of Tax, where Rex modulates Tax expression and reproduction of HTLV-1 (Fig. 1) [110]. The molecular mechanisms in Tax pathogenicity have been clarified and the target molecules of Tax are summarized in Table 2 according to Grassmann *et al.* [23] and Watanabe [106]. Recently, the pathogenicity of HBZ mRNA and protein was analyzed [64, 65]. In addition, Tax, Rex and HBZ proteins are thought to modulate the activation of HTLV-1-proviral DNA and host genes together. Therefore,

Table 2. *Targets and present form of HTLV-1 Tax*

Target	Effect and present form of Tax	References
HTLV-1		
LTR	Direct effect, forming a Tax-CREB-LTR's CRE-motif complex.	[1, 10, 11, 91, 112]
Host cells		
TBP	Direct effect, forming a Tax-CBP complex or a Tax-p300-CAF complex with TBP.	[12, 14]
Signal transduction in host cells		
NF-κB	Direct binding, forming a Tax-IKKg (=NEMO) complex and a Tax-NF-κB-CBP complex	[15, 26, 41, 46]
IL-2 and IL-2 receptor (IL-2R)	Indirect up-regulation	[3, 7, 9, 22, 38, 66, 68, 81, 85]
IL-15 and IL-15 specific receptor (IL-15R)	Indirect activation	[8, 63]
IL-13	Indirect up-regulation	[16, 103]
OX40 and OX40L	Indirect up-regulation	[78]
Transforming growth factor beta 1 (TGF-β1)	Indirect repression	[6, 54, 56]
Kinase-cascades in host cells		
PI3K and its downstream target Akt	Unclear	[60]
ERK-JNK cascade	Unclear	[48, 107]
Cell cycle dysregulation in host cells		
Cdk4, Cdk6 and Cdk2	Direct effect, forming a Tax-Cdk2/4/6 complex	[24, 25, 43, 58, 72, 73]
Cdk inhibitors ($p16^{INK4A}$, $p15^{INK4B}$, $p18^{INK4c}$, $p19^{INK4d}$ and $p27^{Kip1}$)	Direct repression, forming Tax-$p16^{INK4A}$ and -$p15^{INK4B}$ complexes, and indirect suppression ($p18^{INK4c}$, $p19^{INK4d}$ and $p27^{Kip1}$)	[2, 43, 61, 93, 94]
Cyclin E	Indirect up-regulation	[39, 43, 83]
Cyclin D	Indirect up-regulation	[2, 20, 43, 69, 83]
Rb protein	Direct effect, forming a Tax-Rb protein complex	[52, 73]
E2F	Indirect up-regulation	[57, 75]
Cyclin A	Indirect suppression	[53]
ChK 1 and Chk 2	Indirect interaction	[79]
APC	Direct effect, forming a Tax-APC complex	[59]
Cellular checkpoint protein MAD1	Direct effect, forming a Tax-MAD1 complex	[44, 47]
Tumor suppressors and cellular apoptosis in host cells		
p53 and $p21^{Waf1/Cip1}$	Indirect or direct inactivation, forming a Tax-p300/CBP co-activator complex	[5, 102]
hDLG	Direct effect, forming a Tax-hDLG complex	[37, 95]
DNA repair and maintaining chromosomes in host cells		
DNA polymerase β and BER	Indirect suppression	[45]
DNA polymerase δ, NER and mismatch repair.	Indirect suppression	[49]
BclxL that suppresses RAD51 recombination pathway, suppressing homologous recombination.	Induction	[82]
hTERT	Indirect induction	[21, 90]

LTR: Long terminal repeat of HTLV-1 proviral DNA. CREB: Cyclic-AMP-response element binding protein. CRE: Cyclic-AMP responsive. TATA box: Goldberg-Hogness box. TBP: TATA box-bound protein. CBP: CREB-binding protein. CAF: CBP-associated factor. NF-κB: Nuclear factor kappa B. IKKg: I-kappaB-kinase gamma. IKKg=NEMO: NF-κB essential modulator. OX40=CD134: A member of the tumor necrosis factor (TNF)-receptor family and co-stimulatory T-cell molecule. OX40L: OX40 ligand. PI3K: Phosphoinositide 3-kinase. Akt=Protein kinase B (PKB). ERK: Extracellular signal-regulated kinase. JNK: C-Jun NH_2-terminal kinase. Cdk: Cyclin-dependent kinase. Rb protein: Retinoblastoma protein. ChK: Checkpoint kinase. APC: Anaphase promoting complex. hDLG: Human DLG, a homologue of the Drosophila discs large PDZ domain-containing tumor suppressor. BER: Base excision repair. NER: Nucleotide excision repair. hTERT: Human telomerase reverse transcriptase.

the minimum target-molecules in ultra-IHC for etiological diagnosis of ATLL were Tax and Rex, while the histochemistry of HBZ mRNA and protein is currently expected to be established.

a) Modified ImmunoMax/CSA method for Tax and Rex on formalin-fixed paraffin-embedded sections

The rat monoclonal antibody against Tax, WATM-1 [100], mouse monoclonal antibody against Tax, Lt-4 [55], and mouse monoclonal antibody against Rex, Rec-6 [30] were supplied by Dr. Y. Tanaka (Table 3). Sections of the HTLV-1-related cell line MT-2 were obtained from formalin-fixed and paraffin-embedded cell pellets. ATLL formalin-fixed paraffin-embedded sections were archival pathology specimens of lymph nodes diagnosed as ATLL. The modified ImmunoMax/CSA method was performed by a semi-autostainer (MicroProbe™, Fisher Scientific Co.) [30, 31, 62]. Heating-AR was performed, heating sections in 4 M urea solution by pressure cooking for 5 min [30]. Negative control staining was that of the primary antibody reaction employing antibody dilution solution containing no primary antibody.

By means of the heating-AR and ordinary sensitive polymer method (Fig. 2d), only Lt-4 showed faint staining in MT-2 while the other antibodies revealed no staining in MT-2 and ATLL. By means of the heating-AR and modified ImmunoMax/CSA method, in comparison with the negative control (Fig. 3a), MT-2 indicated strong expression of WATM-1-labeled Tax (Fig. 3b) and weak expression of Rec-6-labeled Rex (Fig. 3c). In comparison with the negative control (Fig. 3d), ATLL exhibited weak expression of WATM-1-labeled Tax (Fig. 3e) and obvious expression of Rec-6-labeled Rex (Fig. 3f).

It was suggested that it is possible to detect Tax and Rex on archival pathology specimen sections by means of heating-AR and ultra-IHC. Moreover, it was indicated that there was a difference in Tax and Rex expression pattern between MT-2 and ATLL.

b) Application to case study of ATLL and related lesions

We identified HTLV-1-associated non-neoplastic lymphadenopathy (HANNLA) in HTLV-1 carriers [33]. HANNLA demonstrated atypical follicular hyperplasia, follicle-lysis, and enlarging paracortex associated with somewhat atypical lymphocytes [33]. Atypical follicles were also noted in the tonsil of HTLV-1 carriers [97]. Gradual increased expression of Lt-4 and WATM-1-labeled Tax and high expression of Rec-6-labeled Rex was detected by the heating-AR and modified ImmunoMax/CSA method in atypical lymphocytes in the enlarged paracortex of HANNLA, where marked expression of Ia-like antigen was observed, and an increased number of HTLV-1 proviral DNA copies were estimated semi-quantitatively from polymerase chain reaction (PCR) for HTLV-1 proviral DNA and a host cell gene [30]. It was suggested that HTLV-1-infected non-neoplastic T-cells expressed Tax and Rex in the proliferative lesion, possibly related to occurrence of anti-HTLV-1 immunity.

A smoldering type ATLL manifested as erythema in the bilateral dorsal aspects of the upper arms, the fore chest, the back, the abdomen, and the bilateral anterior aspects of the thigh, and as hyperkeratotic erythema in the bilateral aspects of the toes in a 76-year-old Japanese man. Biopsied erythema in the left aspect of the thigh showed epidermotropism of lymphocytes with their intraepidermal microabscess formation (Fig. 4a), their perivascular infiltration in the upper dermis (Fig. 4b) and their infiltration to hair follicles (Fig. 4c). A biopsied lymph node in the left inguinal region demonstrated dermatopathic lymphadenopathy (DPLA) with hyperplastic lymph follicles and enlarged paracortex (Fig. 4d) where atypical lymphocytes proliferated (Fig. 4e) and comprised $CD4^+$ (Fig. 4f) $CD8^-$ T-cells. Southern blot analysis of DNA extracted from the left inguinal lymph node indicated monoclonal integration of HTLV-1 proviral DNA (Fig. 4j), shown as 1 band in EcoR1 digestion, 3 HTLV-1 proviral DNA bands, and no detection of 2 virus-cellular junction bands in Pst1 digestion. These lesions were diagnosed as that of smoldering ATLL. The heating-AR and modified ImmunoMax/CSA method showed that some ATLL cells proliferating in the paracortex of the left inguinal lymph node expressed weakly WATM-1-labeled Tax (Fig. 4h) and that many of them expressed Rec-6-labeled Rex (Fig. 4i). It was suggested that proliferating ATLL cells in smoldering type expressed Tax weakly and Rex strongly, identical to that of the ATLL in Figure 3.

ATLL initiating in the right palate tonsil and infiltrating to the cervical and axillary lymph nodes was observed in a 51 year-old Japanese woman. She manifested swelling of the right palate tonsil that showed diffuse proliferation of small to medium-sized cells (Fig. 5a and b) with $CD3^+$ $CD4^+$ T-cell phenotype. One month later, a swollen right palate tonsil and right cervical and axillary lymph nodes (Fig. 5c) revealed infiltrative proliferation of medium-sized to large $CD3^+$ $CD4^+$ $CD30^+$ T-cells (Fig. 5d and e) with developing background meshwork of thymidine phosphorylase $(TP)^+$ dendritic cells (Fig. 5f). DNA extracted from the right axillary lymph node indicated oligoclonal integration of proviral DNA, shown as 2 bands in EcoR1 digestion, 3 proviral DNA bands, and 3 weakly labeled virus-cellular junction bands in Pst1 digestion (Fig. 5j), which differed from those of a defective HTLV-1 provirus [23, 99]. Rearrangement of T-cell receptor β was noted (Fig. 5k). This case was an early phase of ATLL developing from small- to medium-sized cells to pleomorphic cells with a $CD30^+$ activating phenotype. In the heating-AR and modified ImmunoMax/CSA method, most ATLL cells in early phase ATLL in the right axillary lymph node showed obvious expression of WATM-1-labeled Tax (Fig. 5h) and much stronger expression of Rec-6-labeled Rex (Fig. 5i) without obvious staining in the negative control (Fig. 5g), suggesting that early ATLL cells with the activating phenotype expressed Tax in an obvious manner.

ATLL was also observed in Native Americans in Argentina [62]. All 5 Native American ATLL cases demon-

Table 3. *Antibodies that appeared in this review*

Antigen	Antibody	Antigen retrieval	Detection method
Used for diagnosis of lymphomas			
CD3	NCL-CD3-PS1, Novocastra	Heating*	Ordinary-IHC #1
CD4	NCL-CD4-IF6, Novocastra	Heating*	Ordinary-IHC #1
CD8	M7103, Dako	Heating*	Ordinary-IHC #1
CD30 (Ber H2)	M0751, Dako	Heating*	Ordinary-IHC #1
Thymidine phosphorylase (TP)	Supplied from Dr. Akiyama S	Heating*	Ordinary-IHC #1
CD5	Leu 1, Becton Dickinson	Heating**	Ultra-IHC #2
Used for detecting HTLV-1 related proteins			
HTLV-1 p40Tax	Mouse mAb, Lt-4, supplied from Dr. Tanaka Y	Heating*, Enzymatic***	Ultra-IHC #2,3
HTLV-1 p40Tax	Rat mAb, WATM-1, supplied from Dr. Tanaka Y	Heating*, Enzymatic***	Ultra-IHC #2,3
HTLV-1 p27Rex	Mouse mAB, Rec-6, supplied from Dr. Tanaka Y	Heating*	Ultra-IHC #2
Used for detecting proliferation, cell cycle and DNA-damaged cell death			
Ki67 antigen (MB-1)	M7240, Dako	Heating*	Ultra-IHC #3
p53	NCL-p53-DO7, Novocastra	Heating*	Ultra-IHC #3
p53 phosphorylated	NCL-p53-PHOS, Novocastra	Heating*	Ultra-IHC #3
E2F-1	sc193, Santa Cruz	Heating**	Ultra-IHC #2
E2F-4	sc511, Santa Cruz	Heating**	Ultra-IHC #2
DP-1	sc610, Santa Cruz	Heating**	Ultra-IHC #2
Cyclin E	NCL-CYCLIN E, Novocastra	Heating**	Ultra-IHC #2
Used for detecting autophagy (autophagic vesicle nucleation)			
Beclin-1	sc11427, Santa Cruz	Enzymatic***	Ultra-IHC #3
Used for detecting stem cells, fetal cells, cancer cells and lymphoma cells			
Survivin	ab469, Abcam	Heating****	Ordinary-IHC #1
CD117	NCL-CD117, Novocastra	Heating*	Ultra-IHC #3

*: Antigen retrieval heating in 0.01 M citrate buffer pH 6.
**: Antigen retrieval heating in 4 M urea solution by pressure cooking for 5 to 10 min in a draft.
***: Antigen retrieval treating sections by proteinase K solution for 10–30 min at room temperature.
****: Antigen retrieval heating in Diva Decloaker buffer (Biocare Medical) independent from pH of solution.
#1: Ordinary-IHC, super sensitive indirect enzyme-labeled antibody method (enzyme- and secondary antibody-labeled polymer reagent method).
#2: Ultra-IHC (Modified ImmunoMax/CSA method, possibly new simplified CSA system and Dako CSA II system modified according to the new simplified CSA system).
#3: Ultra-IHC (New simplified CSA system).

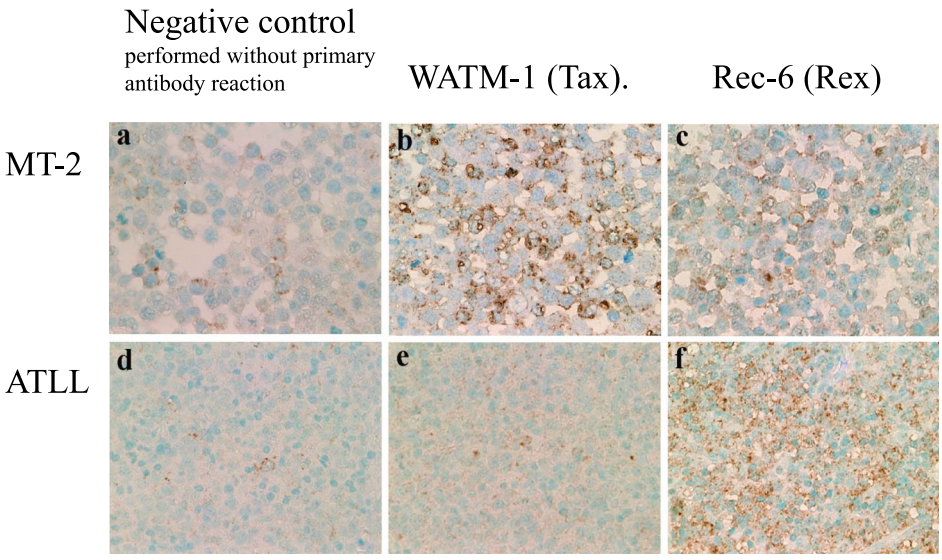

Fig. 3. The modified ImmunoMax/CSA method of Tax and Rex on paraffin sections of MT-2 and 1 case of lymphoma type ATLL (DAB-H_2O_2 reaction with methyl green nuclear counterstaining. ×40, Olympus BX50, FUJIFILM HC-300). **a–c**) MT-2. **d–f**) ATLL. **a** and **d**) Negative control staining performed with antibody dilution fluid containing no primary antibody. **b** and **e**) WATM-1 (Tax). **c** and **f**) Rec-6 (Rex). In comparison with the negative control staining (**a, d**) MT-2 cells show stronger Tax staining (**b**) than ATLL (**e**) does, although ATLL cells show stronger Rex staining (**f**) than MT-2 (**c**) does.

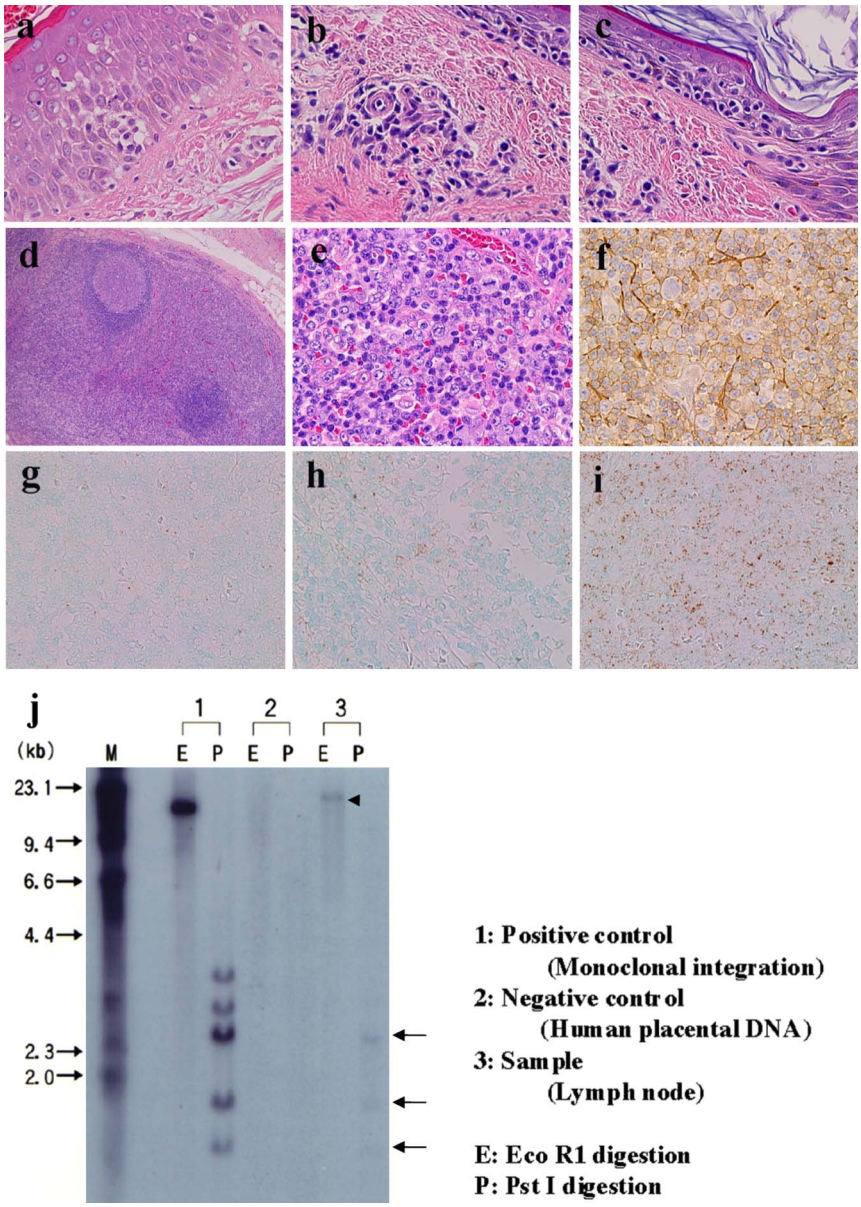

Fig. 4. Tax and Rex Expression in smoldering type ATLL (×40, Olympus BX50, FUJIFILM HC-300). **a–e**) Haematoxylin & Eosin (H.E.). **a–c**) The left thigh showed intra-epidermal microabscess formation (**a**) and infiltration of small atypical lymphocytes around capillaries in the upper dermis (**b**) and into the hair follicle (**c**). **d–i**) The left inguinal lymph node. **d**) Low power view (×10). **e**) High power view of the enlarged paracortex. **f**) Ordinary-IHC of CD4 (DAB-H_2O_2 reaction and haematoxylin nuclear counterstaining). The left inguinal lymph node demonstrates dermatopathic lymphadenopathy, of which the enlarged paracortex (**d**) indicates proliferation of atypical lymphocytes (**e**) positive for CD4 (**f**). **g–i**) The modified ImmunoMax/CSA method (DAB-H_2O_2 reaction with methyl green nuclear counterstaining) for negative control performed without primary antibody (**g**), WATM-1 for Tax (**h**), and Rec-6 for Rex (**i**). In comparison with the negative control staining (**g**) some cells express Tax (WATM-1) weakly (**h**) and many cells express Rex (Rec-6) strongly (**i**). **j**) Southern-blot analysis of HTLV-1 proviral DNA integration. 1) Positive control (ATLL cell line), 2) Negative control (human placental DNA), and 3) DNA extracted from the left inguinal lymph node. E) EcoR1 digestion. Two DNA sequence (GAATTC) in cellular DNA on both ends of the HTLV-1 proviral DNA are digested. P) Pst1 digestion. The DNA sequence (CTGCAG) in HTLV-1 proviral DNA and in cellular DNA on both ends of the HTLV-1 proviral DNA is digested into 3 proviral DNA bands of 1.2 kb, 1.8 kb, 2.5 kb and 2 virus-cellular junction bands. Positive control (1: Monoclonal integration of HTLV-1 proviral DNA in ATLL cell line) shows 1 band labeled by a whole HTLV-1 proviral DNA probe in EcoR1 digestion and 3 proviral DNA bands and 2 virus-cellular junction bands in Pst1 digestion. The DNA extracted from the left inguinal lymph node (3) indicates 1 weak band in EcoR1 digestion (arrow-head) and 3 weak bands of 1.2 kb, 1.8 kb, 2.5 kb in Pst1 digestion (arrows) while 2 virus-cellular junction bands are not recognized, suggesting monoclonal integration of HTLV-1 proviral DNA in some atypical cells.

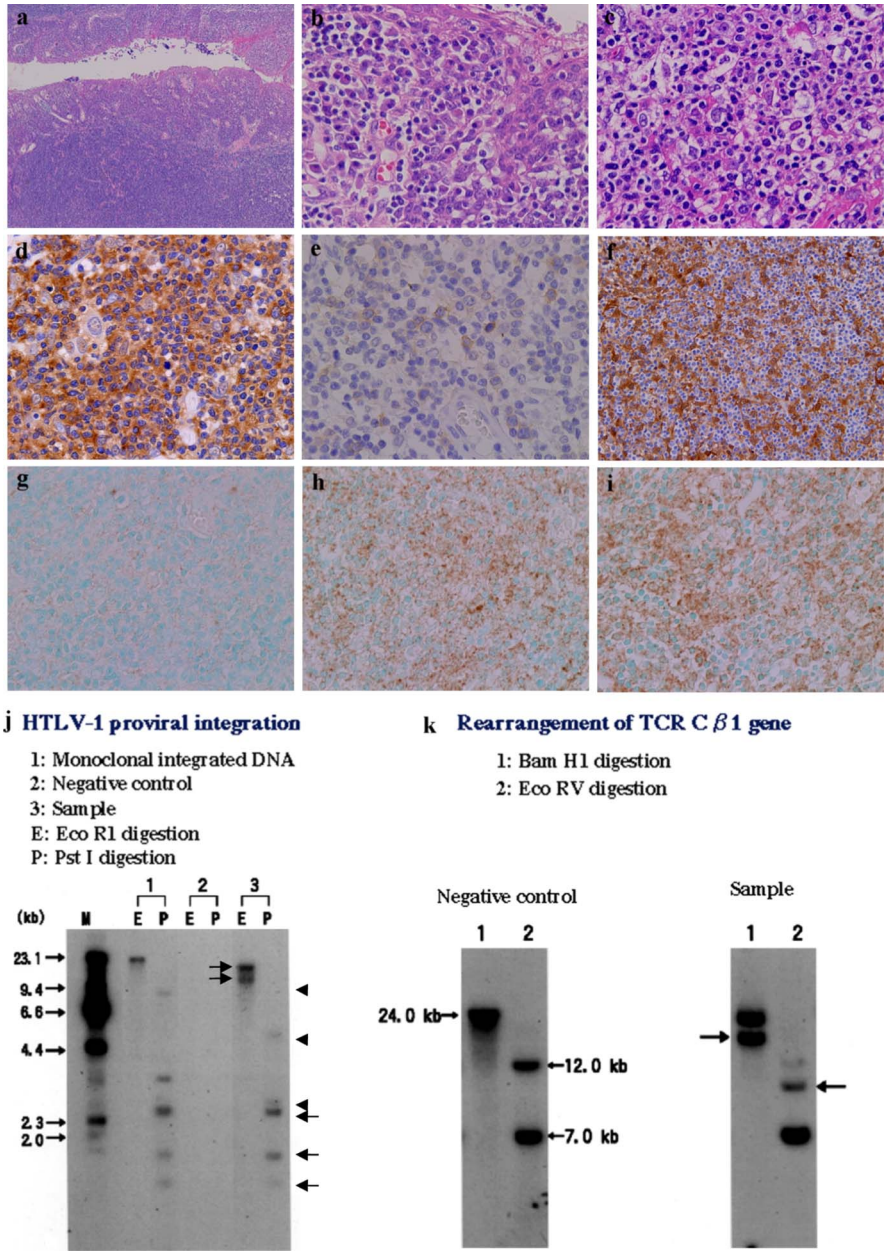

Fig. 5. Tax and Rex expression in ATLL that initiated in the right palate tonsil and infiltrated to the cervical and axillary lymph nodes (×10 or ×40, Olympus BX50, FUJIFILM HC-300). **a** and **b**) First biopsy of the right palate tonsil (H.E.) showing diffuse proliferation of medium-sized ATLL cells (**a**, ×10) and their tropism to the tonsillar epithelia (**b**). **c–i**) Second biopsy of the right axillary lymph node. **c**) Diffuse proliferation of pleomorphic ATLL cells can be observed (H.E.). **d–f**) Ordinary-IHC of CD4 (**d**), CD30 (**e**) and thymidine phosphorylase (TP, **f**) (DAB-H_2O_2 reaction and haematoxylin nuclear counterstaining). Most of the pleomorphic ATLL cells are CD4 T-cells (**d**), some of them express CD30 (**e**), and associate symbiotic growth of TP-positive dendritic cells forming a meshwork. **g–i**) The modified ImmunoMax/CSA method for the negative control (**g**), WATM-1 for Tax (**h**), and Rec-6 for Rex (**i**) (DAB-H_2O_2 reaction and haematoxylin nuclear counterstaining). In comparison with the negative control staining (**g**), expression of Tax (WATM-1) (**h**) and strong expression of Rex (Rec-6) (**i**) are detected in the pleomorphic ATLL cells. **j**) Southern-blot analysis of HTLV-1 proviral DNA integration. 1) Positive control (ATLL cell line), 2) Negative control (human placental DNA), and 3) Sample: DNA extracted from the left axillary lymph node. E) EcoR1 digestion. P) Pst1 digestion. The extracted DNA shows 2 DNA bands from EcoR1 digestion, and 3 proviral DNA bands (arrows) and 3 virus-cellular junction bands (arrow heads) from Pst1 digestion, suggesting oligoclonal integration of proviral DNA in the ATLL cells. **k**) Southern-blot analysis of T-cell receptor β (TCR β). 1) BamH1 digestion. BamH1 digests the DNA sequence (GGATCC) in cellular DNA on both sides of the TCR β DNA sequence. 2) EcoRV digestion. EcoRV digests the DNA sequence (GAATTC) in the TCR β DNA sequence. A rearranged TCR β band is observed in BamH1 (arrow) and EcoRV digestion (arrow) of the sample, suggesting that these pleomorphic ATLL cells are monoclonal αβ T-cells.

Table 4. *Evaluation of E2F, DP-1 and cyclin E in MT-2, ATLL and peripheral T-cell lymphomas in Europeans (EPTL), detected by the heating-AR and modified ImmunoMax/CSA method*

	HTLV-1			E2F		DP-1	Cyclin E
	Proviral DNA	Tax	Rex	E2F-1	E2F-4		
MT-2	integrated	+++	++	–	++	+++	–
ATLL 1	integrated	+	+++	–	+++	+++	++
ATLL 2	integrated	+	+++	–	–	+++	++
ATLL 3	integrated	+	++	–	–	++	++
ATLL 4	integrated	+	++	–	–	++	++
ATLL 5	integrated	+/–	++++	+	–	++	+
ATLL 6	integrated	+/–	++	–	–	+/–	–
ATLL 7	integrated	+/–	++	–	–	++	+
ATLL 8	integrated	–	+++	+++	–	+++	+
ATLL 9	integrated	–	+++	–	++	–	+
EPTL 1	n.e.	n.e.	n.e.	+++	+++	++	++
EPTL 2	n.e.	n.e.	n.e.	++	+/–	+++	+++
EPTL 3	n.e.	n.e.	n.e.	++	+	+++	+++
EPTL 4	n.e.	n.e.	n.e.	+	+/–	++	+++
EPTL 5	n.e.	n.e.	n.e.	+	–	+++	++
EPTL 6	n.e.	n.e.	n.e.	+/–	+/–	+++	+++
EPTL 7	n.e.	n.e.	n.e.	–	+/–	+++	+++
EPTL 8	n.e.	n.e.	n.e.	+/–	–	+++	++
EPTL 9	n.e.	n.e.	n.e.	–	–	+++	+

ATLL: Adult T-cell leukemia, lymphoma type. EPTL: Peripheral T-cell lymphoma in European, diagnosed in Dept. of Pathology (Prof. Martin-Leo Hansmann), Johann Wolfgang Goethe-Universität Frankfurt am Main.
[HTLV-1 proviral DNA] Integrated: HTLV-1 proviral DNA was shown to be integrated in lymphoma cells. n.e.: Not examined.
Evaluation of the immunostainig of the modified ImmunoMax/CSA method of Tax, Rex, E2F-1, E2F-4, DP-1, and Cyclin E. –: Not positive cells. +/–: Rare very weakly positive cells. +: A few weakly positive cells. ++: Some moderately positive cells. +++: Many strongly positive cells. ++++: Almost all very strongly positive cells. n.e.: Not examined.
ATLL Tax vs. Cyclin E: Wilcoxon signed-ranks test, p=0.0209.

strated obvious Tax and strong Rex expression, respectively, in archival sections of pathology specimens tested by the heating-AR and modified ImmunoMax/CSA method using WATM-1 and Rec-6 [62]. However, 2 of 9 Kagoshima ATLL cases did not demonstrate positive staining of WATM-1-labeled Tax with the heating-AR and modified ImmunoMax/CSA method (Table 4).

Clinically, approximately half of all ATLL cases are leukemia, and the patients' lymph nodes were usually not examined pathologically. A lump of naturally precipitated and coagulated peripheral blood can be processed into a formalin-fixed and paraffin-embedded specimen, i.e., peripheral blood tissue specimen (PBTS) [35]. Leukemic ATLL cells in the PBTS can be examined in the same manner as those in archival pathology specimens. In PBTS of 6 of 8 leukemic type ATLL cases comprising 4 chronic and 4 acute leukemia type cases, Tax and Rex were detected weakly and strongly, respectively, in a few or some ATLL cells with the heating-AR and modified ImmunoMax/CSA method using WATM-1 and Rec-6 [35].

HTLV-1-infected T-cells in the proliferative lesion in the paracortex of HANNLA and ATLL cells proliferating in the paracortex of DPLA in smoldering ATLL and in the lymph nodes in early phase lymphoma type ATLL and in lymphoma type ATLL in Native Americans and in Japanese (Kagoshima natives) expressed Tax weakly and Rex strongly with the heating-AR and modified ImmunoMax/CSA method. Tax expression was correlated to Ki67 antigen$^+$ proliferating cells in PBTS of leukemia type ATLL [35]. A present form of Tax retrieved by heating AR and detected with the modified ImmunoMax/CSA method of WATM-1 against Tax may be related with ATLL cell proliferation.

c) Enzymatic-AR and ultra-IHC of Tax

Tax is synthesized from the integrated HTLV-1 proviral DNA pX region. As listed in Table 2, Tax forms a complex with cyclic-AMP-response element binding protein (CREB), docks at cyclic-AMP responsive (CRE)-motifs of the HTLV-1 proviral DNA long terminal repeat (LTR) and up-regulates Tax synthesis [1, 10, 11, 42, 91, 112]. On the other hand, Tax binds directly TATA box-bound protein (TBP), recruits CREB-binding protein (CBP), p300 and p300/CBP-associated factor (P/CAF) and forms Tax-CBP-p300 and Tax-P/CAF complexes [12, 14], trans-activating or -suppressing host cells genes. Besides, Tax binds directly I-kappaB-kinase gamma (IKKg, =NEMO: NF-κB essential modulator) and indirectly up-regulation of Nuclear factor kappa B (NF-κB), effecting down-stream

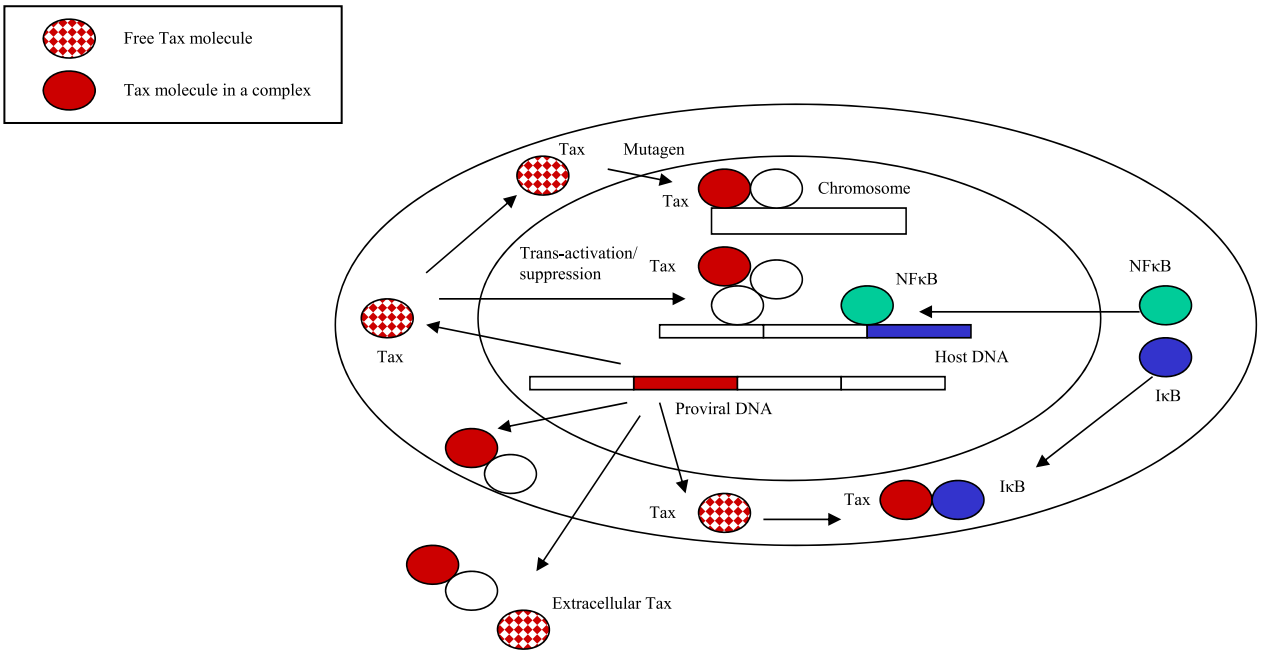

Fig. 6. Present forms of Tax in a HTLV-1 infected T-cell. Tax is synthesized in the cytoplasm based on spliced one of RNAs from the HTLV-1 proviral DNA, often binding other molecules such as IκB in the cytoplasm and cAMP responsive element binding (CREB), DNA, and chromosomes in the nucleus to manifest its pathogenicity. There are at least 2 present forms of Tax, a simple form existing freely or in a simple complex with other molecules, and a complex form forming a complicated complex with other molecules.

signal transductions and their products [15, 26, 41, 46]. Tax binds directly cyclin-dependent kinases 2, 4, and 6 (Cdk2, Cdk4 and Cdk6) [24, 25, 43, 58, 72, 73] and Cdk inhibitors ($p16^{INK4A}$ and $p15^{INK4B}$) and indirectly suppresses the other Cdk inhibitors ($p18^{INK4c}$, $p19^{INK4d}$, and $p27^{Kip1}$) [2, 43, 61, 93, 94]. Tax binds also directly retinoblastoma (Rb) protein [52, 73], anaphase promoting complex (APC) [59], cellular checkpoint protein MAD1 [44, 47], and human DLG, a homologue of the Drosophila discs large PDZ domain-containing tumor suppressor [37, 95]. There are at least 2 present forms of Tax, a simple present form (Free Tax molecule, Fig. 6) and a complex present form (Tax molecule in a complex, Fig. 6) that comprises the complicated complexes mentioned above (Fig. 6). The efficiency of AR on antigens in the Tax molecule may depend on its present form in HTLV-1-infected T-cells. Heating-AR in the modified ImmunoMax/CSA method of WATM-1 would expose the simple present form of Tax to the anti-Tax antibody WATM-1. On the other hand, enzymatic-AR digests the simple present form of Tax, some molecules masking Tax in the complicated complexes and tissues around Tax to expose Tax to the primary antibody, as suggested in ultra-IHC of beclin-1 (Table 3) [50, 104]. In order to detect the complex form of Tax, we employed enzymatic-AR treating sections with 200 μg/mL proteinase K solution for 10–30 min at room temperature and nsCSA system (Table 1C, Fig. 2g) [28, 34].

The enzymatic-AR and nsCSA system (Table 1Ca) visualized immunostaining that was more obviously granular with Lt-4 than with WATM-1 in some lymphocytes of HTLV-1 carriers (Fig. 7a and b) and ATLL cells (Fig. 7c–f) in PBTS. Chronic leukemia type ATLL (Fig. 7c and d) exhibited granular Lt-4 immunostaining in more cells than HTLV-1 carriers (Fig. 7a and b) and acute leukemia type ATLL (Fig. 7e and f) (Table 5, Kruskal-Wallis test, $p=0.0388$). Chronic ATLL cells may depend more on Tax than acute type ATLL cells and HTLV-1-infected cells in HTLV-1 carriers, suggesting the possibility that Tax maintains chronic type ATLL cells. However, non-specific dense nuclear staining with Lt-4 and WATM-1 was observed in an acute myelogenous leukemia (AML) patient without antibodies against HTLV-1 (Fig. 7g and h). Based on hematological diagnosis of peripheral T-cell leukemia, HTLV-1 infection in leukemic cells could be detected in PBTS by the enzymatic-AR and nsCSA system of Lt-4 for Tax. Peripheral T-cell leukemia with Lt-4-labeled leukemia cells has to be diagnosed as ATLL.

The enzymatic-AR and nsCSA system of Lt-4 was applied to paraffin sections of 29 malignant lymphoma cases diagnosed in a hospital's Department of Pathology. Thirteen of 14 PTCL cases were diagnosed pathologically as ATLL based on clinical information regarding anti-HTLV-1 antibodies in the serum or the integration of HTLV-1 proviral DNA in lymphoma cells (Table 6).

As shown in Figure 8, a small number of ATLL cells displayed obvious granular Lt-4 staining in all 13 ATLL cases. Pleomorphic large lymphoma cells of PTCL not-otherwise specified (PTCL NOS) displayed obvious granular Lt-4 staining (Fig. 8b). Since the Lt-4 immunostaining provided information regarding HTLV-1 infection, this

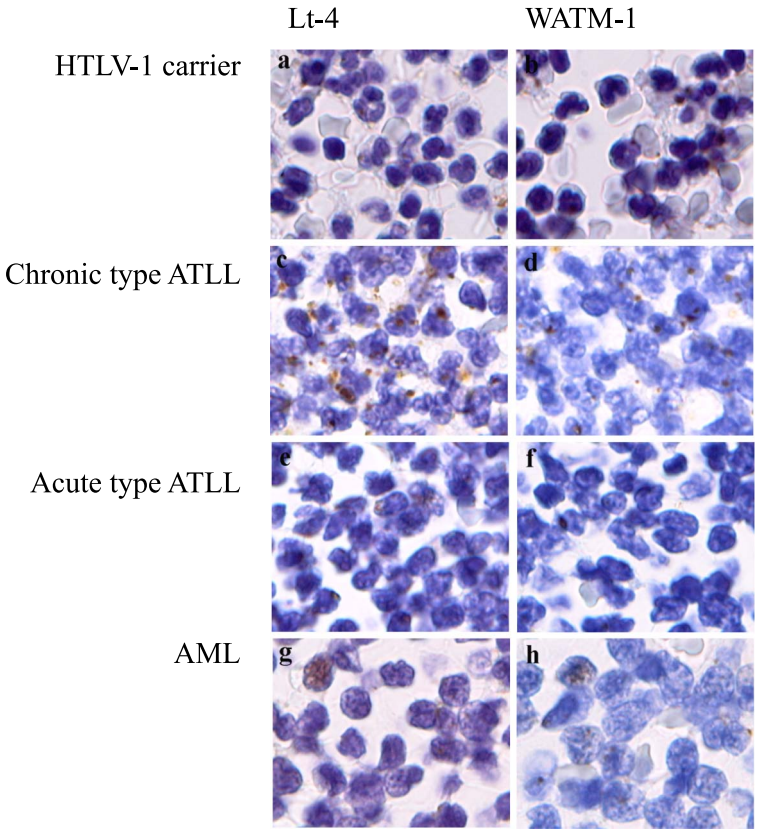

Fig. 7. Tax expression detected by the enzymatic-AR and nsCSA system in peripheral blood tissue specimen (PBTS) (DAB-H_2O_2 reaction and haematoxylin nuclear counterstaining, ×100 oil (×2.5 digital), Olympus BX50, FUJIFILM HC-300). **a** and **b**) HTLV-1 carrier. **c** and **d**) Chronic type ATLL. **e** and **f**) Acute type ATLL. **g** and **h**) Acute myelogenous leukemia (AML). More obvious granular immunostaining is seen in Lt-4 (**a, c** and **e**) than in WATM-1 (**b, d** and **f**) in HTLV-1 carriers, and chronic and acute type ATLL. However, nuclear staining by Lt-4 (**g**) and WATM-1 (**h**) is noted in an AML patient without antibodies against HTLV-1.

Table 5. *Enzymatic-AR and new simplified CSA system of Lt-4 against Tax in PBTS of HTLV-1 carriers, ATLL and the other leukemias*

	Positive cells in PBTS			
	No positive cells	A few positive cells	Some positive cells	Many positive cells
HTLV-1 carrier*	0	0	2	0
Chronic type ATL*	0	0	4	3
Acute type ATL*	0	3	3	0
The other leukemias	2	0	3**	0

*: Kruskal-Wallis test, p=0.0388. **: Nuclear staining in some cells.

PTCL NOS could be diagnosed as ATLL. The enzymatic-AR and nsCSA system of Lt-4 was informative for HTLV-1 infection even in cases dominated by medium-sized cells (Fig. 8e). In an ATLL case, a medium-sized cell exhibited granular Lt-4 immunostaining localized in the cytoplasm, and a large cell facing the medium-sized cells revealed faint Lt-4 immunostaining in the cytoplasm (Fig. 8f). This figure possibly suggested an image of HTLV-1 infection through viral synapse [40]. The positive immunostaining of the enzymatic-AR and nsCSA system of Lt-4 in background cells (Table 6) suggested a possibility of secondary ATLL from other lymphomas [32, 74], especially Hodgkin lymphomas [74].

Non-specific immunostaining in the enzymatic-AR and nsCSA system of Lt-4 was noted in 11 cases of B-cell neoplasm/malignant lymphoma (BML) (Table 6) and could be differentiated from the specific granular Lt-4 immunostaining in ATLL. Nuclear staining was observed in 5 cases of follicular lymphomas (FL, Fig. 9a) and in 1 case of B-cell chronic lymphocytic leukemia (B-CLL), as well as in PBTS of AML (Fig. 7g). Cytoplasmic fine staining was observed in 1 case each of FL and diffuse large B-cell lymphoma (DLBCL, Fig. 9b). Nucleolar staining was observed in 2 DLBCL cases (Fig. 9c). In addition, dense, clustered granule-like cytoplasmic staining was observed in 1 case of lymphoplasmacytic lymphoma (LP, Fig. 9d).

The non-specific nuclear staining in the enzymatic-AR and nsCSA system of Lt-4 and WATM-1 may have been that of the primary antibody. It may be possible to diminish the nuclear staining by employing Protein block containing 8% horse serum as was done with the modified ImmunoMax/CSA method. However, the modified ImmunoMax/

Table 6. *Enzymatic-AR and new simplified CSA system of Lt-4 applied to paraffin sections of malignant lymphomas*

		Immunostaining		
	n	Negative	Positive background cells	Positive lymphoma cells
T/NK-cell neoplasm (TML)	16	0	2	14
ATLL	13	0	0	13
PTCL, NOS	1	0	0	1
EATL	1	0	1	0
Extranodal NKTCL	1	0	1	0
B-cell neoplasm (BML)	12	1	0	11#
FL	7	1	0	6#
DLBCL	3	0	0	3#
LP	1	0	0	1#
B-CLL	1	0	0	1#
Hodgkin lymphoma (HD)				
Mixed cellularity classic HD	0	0	1	0
Total	29	1	3	25 (11#)

[T/NK-cell neoplasm/malignant lymphoma: TML] ATLL: Adult T-cell leukemia/lymphoma. PTCL, NOS: Peripheral T-cell lymphoma, not-otherwise specified. EATL: Enteropathy-associated T-cell lymphoma. Extranodal NKTCL: Extranodal NK/T-cell lymphoma.
[B-cell neoplasm/malignant lymphoma: BML] FL: Follicular lymphoma. DLBCL: Diffuse large B-cell lymphoma. LP: B-cell lymphoplasmacytic lymphoma. B-CLL: B-cell chronic lymphocytic leukemia.
#: Non-specific immunostaining was noted in 11 cases of BML in total. Non-specific nuclear staining was seen in 5 FL and 1 B-CLL. Non-specific nucleolar staining was in 2 DLBCL. Non-specific cytoplasmal fine staining was in 1 FL and 1 DLBCL. Non-specific cytoplasmal dense staining was in 1 LP.

CSA method of Lt-4 labeled the nuclei of epidermal squamous cells [31]. Since nuclear staining, differing from the granular staining in the nucleus, was often seen in leukemia and lymphoma other than ATLL, such Lt-4 and WATM-1 nuclear staining would not be related to HTLV-1 pathogenicity.

The nucleolar and cytoplasmic non-specific immunostaining in BML was thought to be that of the secondary antibody reagent, although rare HTLV-1-related BML might exist. The secondary antibody reagent is usually goat polyclonal antibodies against immunoglobulin (Ig) G1 from a species of the primary antibody, and often includes a relatively low amount of antibodies against IgG Fc region and BSA (Hapten carrier protein). Nucleolar and cytoplasmic non-specific immunostaining would be diminished if Protein block employing a solution of 8% serum from the secondary antibody species (PBS containing 8% goat serum and 0.25% casein) was carried out prior to the HRP- and secondary antibody-labeled polymer reagent reaction (step 10 in Table 1C). On the other hand, an affinity-purified secondary antibody reagent is also expected to diminish nucleolar and cytoplasmic non-specific immunostaining in the nsCSA system employing the serum-free Protein block.

The obvious granular immunostaining in the enzymatic-AR and nsCSA system of Lt-4 was thought to be pathognomonic for ATLL. Thus, the enzymatic-AR and nsCSA system of Lt-4 was expected to be a useful tool for the etiological pathological diagnosis of ATLL, considering the pathogenicity of Tax.

IV. Application of Ultra-IHC to Analysis of ATLL Oncogenesis and Pathogenesis

Oncogenesis and pathogenesis of ATLL can be understood conceptually from the viewpoint of HTLV-1 pathogenicity, as shown in Figure 1. HTLV-1 pathogenicity has usually been investigated by means of molecular biology/virology and fruitful results have been reported. It is also studied from a genetic immunological viewpoint because ATLL develops in a host that is immunologically compromised against HTLV-1 infection. It is usually difficult to examine pre-neoplastic phase and early-phase lesions of ATLL pathologically. However, fortunately, as mentioned above, we were able to carry out trials to detect HTLV-1 related molecules by means of ultra-IHC in HANNLA, smoldering ATLL, early phase ATLL and developed/lymphoma type ATLL. Moreover, we developed the PBTS method [35] to prepare sections of peripheral blood mononuclear cells (PBMCs) for IHC. Thus, we were able to examine PBMCs in HTLV-1 carriers and leukemic ATLL cells.

We recognized HANNLA [33] as displaying atypical follicular hyperplasia with irregularly-shaped germinal centers (GCs) and enlarged paracortex. It is possible that some HTLV-1-infected regulatory T-cells were related to the irregularly-shaped GCs [33, 97]. In the enlarged paracortex, atypical lymphocytes expressed Tax weakly and Rex strongly with Ia-like antigen$^+$ cells, while the extracted DNA suggested increased copies of HTLV-1 proviral DNA, suggesting that the enlarged paracortex of HANNLA was

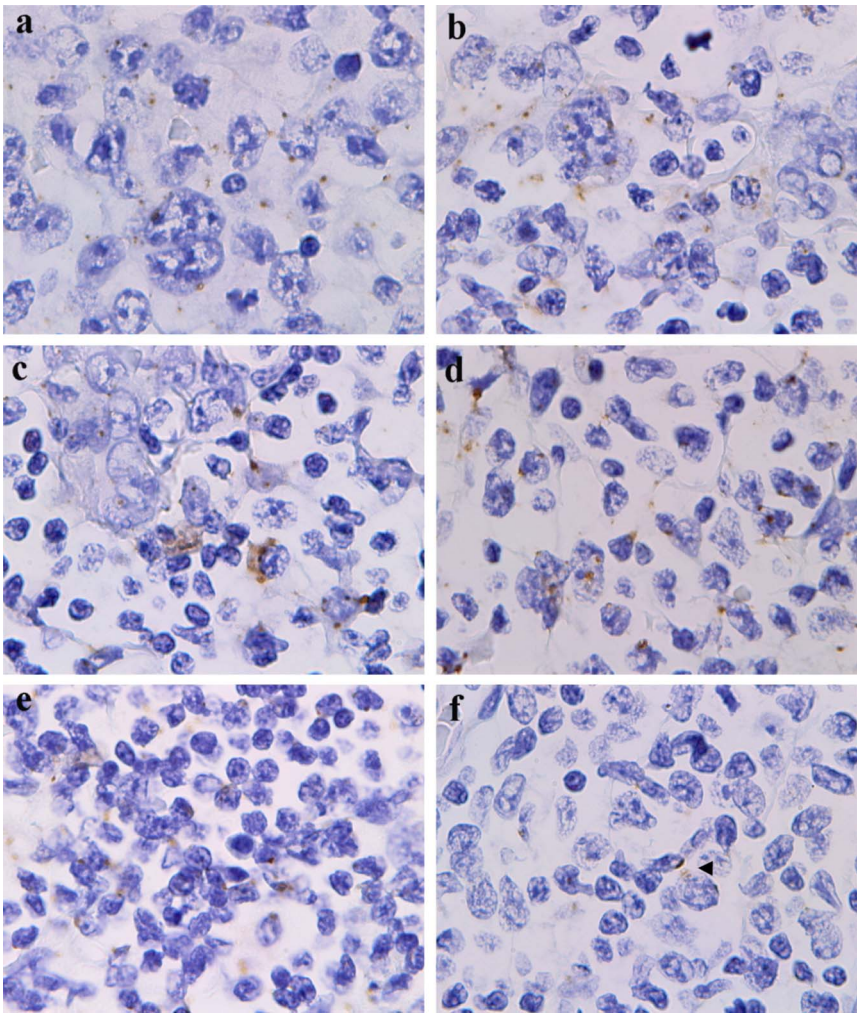

Fig. 8. Tax expression detected by the enzymatic-AR and nsCSA system of Lt-4 in archival paraffin specimens of peripheral T-cell lymphomas with and without clinical information regarding HTLV-1 infection (ATLL and PTCL) (DAB-H_2O_2 reaction and haematoxylin nuclear counterstaining, ×100 oil, Olympus BX50, FUJIFILM HC-300). More or less granular Lt-4 staining is noted in the nucleus and cytoplasm. Variously-sized pleomorphic lymphoma cells in ATLL (**a, c–e**) and PTCL (**b**) show dominantly intranuclear granular Lt-4 staining. Medium-sized and large ATLL cells show cytoplasmic Lt-4 staining in cells facing one another (**f**, arrow head). As Lt-4 staining in PTCL cells (**b**) provides immunohistochemical information of HTLV-1 infection, this case might be diagnosed pathologically as ATLL.

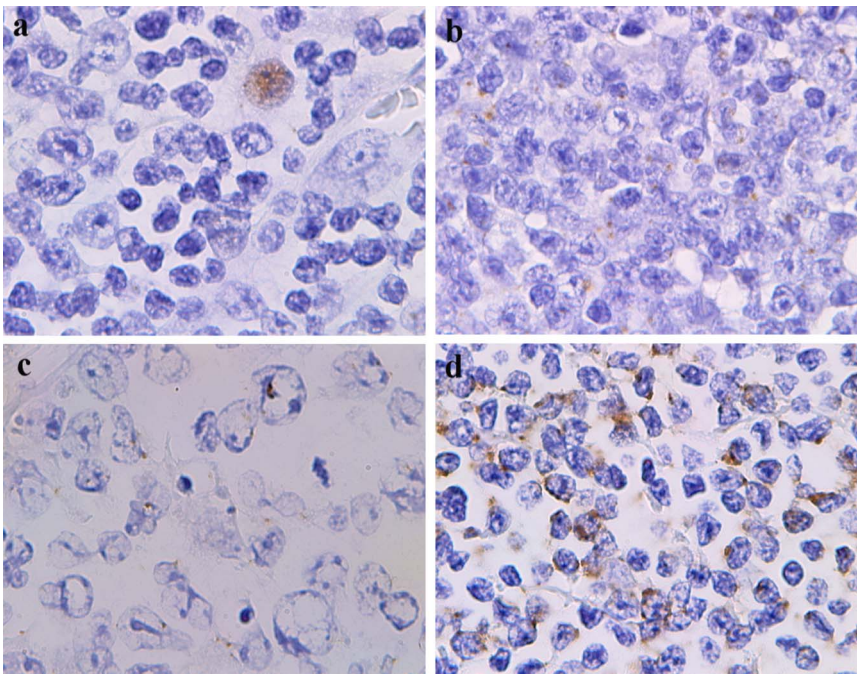

Fig. 9. Non-specific staining in the enzymatic AR and nsCSA system of Lt-4 in archival paraffin specimens of B-cell neoplasms (DAB-H_2O_2 reaction and haematoxylin nuclear counterstaining, ×100 oil, Olympus BX50, FUJIFILM HC-300). **a**) Nuclear staining in follicular lymphoma (FL). **b**) Fine granular staining in diffuse large B-cell lymphoma (DLBCL). **c**) Nucleolar staining in DLBCL. **d**) Dense cytoplasmic staining in lymphoplasmacytic lymphoma/immunocytoma (LP).

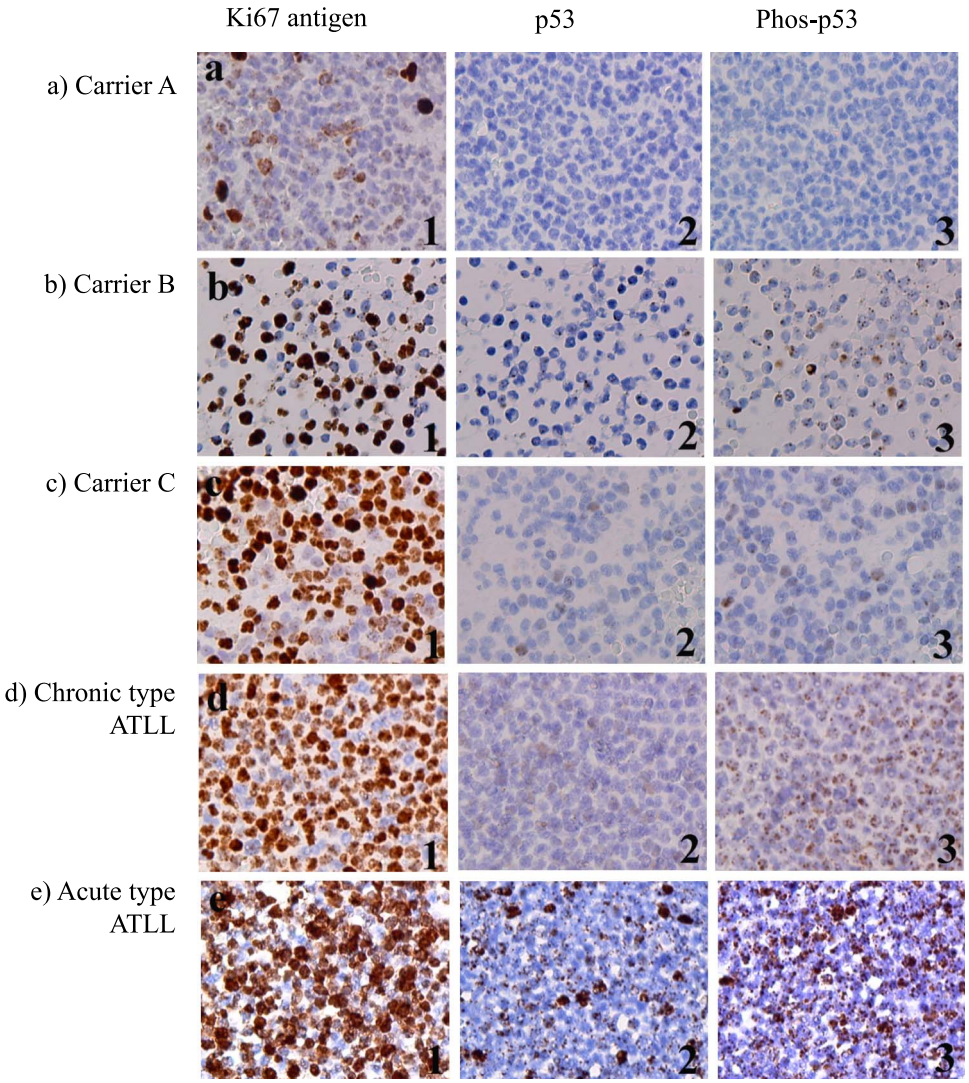

Fig. 10. Expression of Ki67 antigen, p53 protein (p53) and phosphorylated p53 protein (phos-p53) detected by the heating-AR and nsCSA system on the PBTS of HTLV-1 carriers and ATLLs (DAB-H_2O_2 reaction and haematoxylin nuclear counterstaining, ×40 and digital ×2, Olympus BX50, FUJIFILM HC-300). **a–c**) HTLV-1 carriers. **d**) Chronic type ATLL. **e**) Acute type ATLL. 1) Ki67 antigen. 2) p53. 3) phos-p53. Gradual increase of Ki67 antigen$^+$ cells in PBTS is noted in HTLV-1 carriers (**a1–c1**) and most of chronic and acute type ATLLs. Most leukemic ATLL cells were positive for Ki67 antigen (**d1** and **e1**). Physiological expression of p53 in the cytoplasm and nucleus is detected by the heating-AR and nsCSA system in HTLV-1 carriers (**c2**) and chronic type ATLL (**d2**), while dense nuclear expression of probable mutated p53 is noted in acute type ATLL (**e2**), suggesting the possibility of differentiating acute from chronic type ATLL by detecting dense nuclear expression of p53. On the other hand, phos-p53 is observed in HTLV-1 carriers (**b3** and **c3**) and ATLL (**d3** and **e3**), suggesting the possibility of detecting HTLV-1 proviral DNA activity to inactivate p53-mediated DNA damage-induced cell death, since HTLV-1 inactivates p53 by phosphorylating Ser392 in its non-specific DNA binding or oligomerization domains. The immunostaining of p53 in **b2** is similar to that of phos-p53 in **b3**, indicating that phosphorylated p53 is detected by the anti-p53 antibody, and is different from that in **c2**. Thus, the immunostaining of p53 in **b2** is evaluated as negative.

the site where occurred anti-HTLV-1 immunity and expansive HTLV-1 infection in the atypical lymphocytes [30] that maintained a viral load in PBMCs. Tax (Lt-4 or WATM-1)-positive lymphocytes in the PBTS of HTLV-1 carriers (Fig. 7a and b) may be HTLV-1-infected T-cells circulating from HANNLA-like lesions in the lymphoreticular system.

It is difficult to label individual early neoplastic HTLV-1-infected T-cells but IHC of survivin (Table 3) may succeed in this aspect [104]. Mutagens other than Tax, such as APOBEC3G (apolipoprotein B mRNA-editing, enzyme-catalytic, polypeptide-like 3G) [19], would precede neoplastic changes such as over-expression of TSLC1 (tumor suppressor in lung cancer 1) [84] independently from Tax in pre-ATLL cells. DNA damages induced by such mutagens may be removed by the p53 protein system when HTLV-1 inactivates the p53 protein by phosphorylating it [80], and Tax abrogates p53-induced cell cycle arrest and apoptosis through its CREB/activating transcription factor (ATF)

functional domain [70], prevents repair of damaged DNA by suppressing DNA polymerases β [45] and δ [49] and BclxL [82] (Table 2). It is well known that mutated p53 protein that has accumulated in the nucleus is detected by ordinary-IHC in archival pathology specimens. We wanted to observe physiological expression of p53 protein so that we examined Ki67 antigen (Table 3) for proliferating cells, p53 protein and p53 protein phosphorylated at Ser392 in non-specific DNA binding domain (phos-p53) (Table 3) in PBTS of HTLV-1 carriers and ATLL by means of the heating-AR and nsCSA system (Fig. 10). A gradual increase of Ki67 antigen$^+$ proliferating cells and gradual enhanced expression of p53 protein and phos-p53 were observed in HTLV-1 carriers. The gradual increase of Ki67 antigen$^+$ proliferating cells might be due to the effects of Tax and HBZ mRNA [64, 65] in PBMCs of HTLV-1 carriers. Weak detection of p53 protein was dominant in the PBMCs' cytoplasm of HTLV-1 carriers (Fig. 10 c2) and chronic type ATLL (Fig. 10 d2). This weak cytoplasmic immunostaining of the p53 protein was believed to be its physiological expression. Dense nuclear staining of the p53 protein, probably a mutant p53 protein, was observed in acute type ATLL (Fig. 10 e2) as reported previously [105], suggesting a possible standpoint for bone marrow transplantation therapy in acute type ATLL [77]. After categorizing 8 HTLV-1 carriers in to 3 groups, i.e., p53$^-$ phos-p53$^-$ (2 cases, Fig. 10 a2 and a3), p53$^-$ phos-p53$^+$ (3 cases, Fig. 10 b2 and b3) and p53$^+$ phos-p53$^+$ (3 cases, Fig. 10 c2 and c3), we determined that there was a significant difference in age among the 3 groups (mean ages: 32, 45 and 50 years, Kruskal-Wallis test p=0.049), indicating physiological expression of the p53 protein (Fig. 10 c2) against accumulation of DNA damages/mutations according to age and inactivation of p53 by HTLV-1 infection [70, 80]. The immunostaining of p53 protein (Fig. 10 b2) was similar to that of phos-P53 (Fig. 10 b3) in PBMCs in the PBTS of carrier B, but differed from that of the p53 protein (Fig. 10 c2 and d2) in carrier C and chronic type ATLL, suggesting that immunostaining of the p53 protein (Fig. 10 b2) was that of phos-p53. In addition, the appearance of phos-p53 in PBMCs might suggest the initial phase of ATLL oncogenesis, since Tax inactivates the p53 protein by phosphorylating it [70, 80]. Further studies on the expression of neoplastic features such as survivin [13] and human telomerase reverse transcriptase (hTERT) [21, 90] and that of mutagens such as APOBEC3G [19] are necessary to evaluate oncogenetic advances in the p53$^-$ phos-p53$^+$ and p53$^+$ phos-p53$^+$ stages of HTLV-1 carriers. Specific approaches

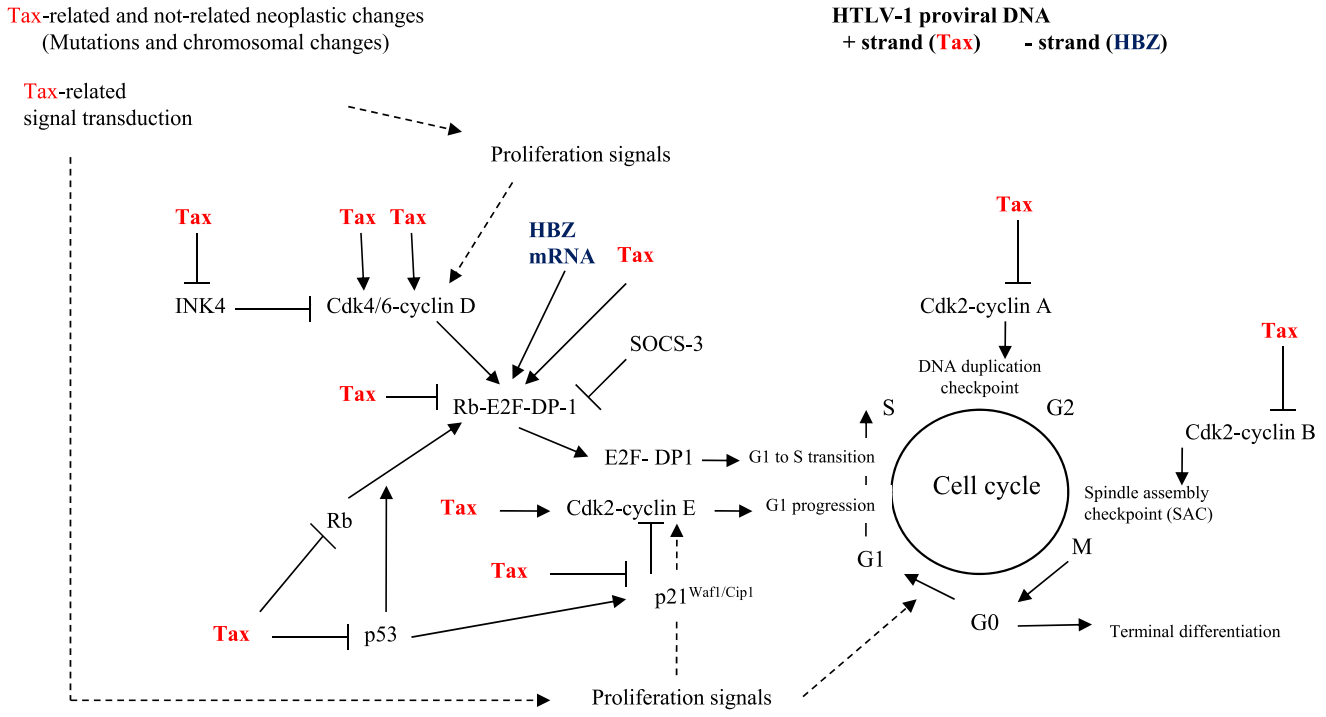

Fig. 11. Effects of Tax and HBZ mRNA molecular mechanism on cell cycle. Tax trans-scripted from the + strand of HTLV-1 proviral DNA trans-activates several genes, targets several molecules in signal transduction as listed in Table 2, and produces proliferation signals to initiate the G1 phase, cyclin E related to G1 progression, and cyclin D related to G1–S transition with stimuli from Tax-related and Tax-unrelated neoplastic changes. Tax suppresses p53, which propels for Rb to form a complex with E2F-DP-1, and suppresses p21$^{Waf1/Cip1}$, which is cyclin-dependent kinase inhibitor 1 suppressing the Cdk2-cyclin E and Cdk4/6-cyclin D complexes. Furthermore, Tax trans-activates E2F-1, trans-suppresses p16^{INK4A}, and stimulates Cdk4/6 into binding with cyclin D to release the E2F-DP-1 complex from the Rb complex to G1–S transition. On the other hand, HBZ mRNA releases E2F-DP-1 to G1–S transition. Tax also degrades cyclin A to propel over-duplication of DNA in the S phase and disrupts cyclin B to upset spindle assembly checkpoint.

to halting Tax in these stages of HTLV-1 infection seems to be warranted because green tea has the effect of reducing viral load in peripheral blood [92].

Expression of the simple present form of Tax detected by heating-AR and modified ImmunoMax/CSA method of WATM-1 was related with proliferation of probable HTLV-1-infected T-cells in HANNLA and in smoldering type, lymphoma type and leukemic ATLL cells, as mentioned above. The molecular mechanisms of Tax, HBZ mRNA and their effect on the cell cycle are illustrated in Figure 11. Tax transcripted from the + strand of HTLV-1 proviral DNA trans-activates several genes [110], targets several molecules in signal transduction as listed in Table 2, and produces proliferation signals to initiate the G1 phase, cyclin E-related to G1 progression, and cyclin D-related to G1–S transition with stimuli from Tax-related and Tax-unrelated neoplastic changes. Tax suppresses p53 [5, 70, 80, 102], blocking Rb [52, 73] to form a complex with E2F-DP-1, and suppresses $p21^{Waf1/Cip1}$, which in turn suppresses the Cdk2-cyclin E complex. Further, Tax trans-activates E2F-1 [110], -suppresses Cdk inhibitors such as $p16^{INK4A}$ [2, 43, 61, 93, 94], and binds Cdk4/6 [24, 25, 43, 58, 72, 73] to bind with cyclin D to release the E2F-DP-1 complex from Rb to G1–S transition, competing with the p53 protein that is inactivated by Tax [70, 80]. DP-1 is stabilized by binding with SOCS-3 in the cytoplasm. On the other hand, HBZ mRNA releases E2F-DP-1 to G1–S transition [64, 65]. Additionally, Tax degrades cyclin A to propel over-duplication of DNA [53] and binds anaphase promoting complex (ABC) to disrupt cyclin B to upset spindle assembly checkpoints [59]. In order to see features in cell cycle in MT-2, 9 cases of lymphoma type ATLL with monoclonal integration of HTLV-1 proviral DNA, and 9 cases of PTCL in Europeans (EPTL) free from HTLV-1 infection, we examined E2F-1 activator and E2F-4 suppressor for G1–S transition, DP-1 [29], and cyclin E with the heating-AR and modified ImmunoMax/CSA method (Table 4). MT-2 expressed E2F-4 in an obvious manner in the nuclei and DP-1 predominantly in the cytoplasm, but not E2F-1 and cyclin E (Fig. 12a–d). ATLL expressed E2F-1 or E2F-4 in the nuclei in spite of weak E2F-1 expression in the cytoplasm of some cells in 1 case (ATLL5 in Table 4), moderate DP-1 expression in the cytoplasm and cyclin E in some cells (Fig. 12g and h, Table 4). In ATLL, Tax expression detected by the heating-AR and modified ImmunoMax/CSA method of WATM-1 revealed correlation with cyclin E expression (Wilcoxon signed-ranks test, $p=0.0209$) but did not suggest any relation to the expression of E2F-1, E2F-4, and DP-1 (Table 4), suggesting that Tax expression was correlated with the proliferation of lymphoma type ATLL cells. EPTL expressed both E2F-1 and E2F-4 in some cells weakly, but expressed DP-1 and cyclin E strongly in most cells (Fig. 12i to l, Table 4). The expression of E2F-1 and E2F-4 in EPTL was quite different from that in ATLL and had no correlation with that of cyclin E (Table 4). The molecular mechanism in the G1–S phase

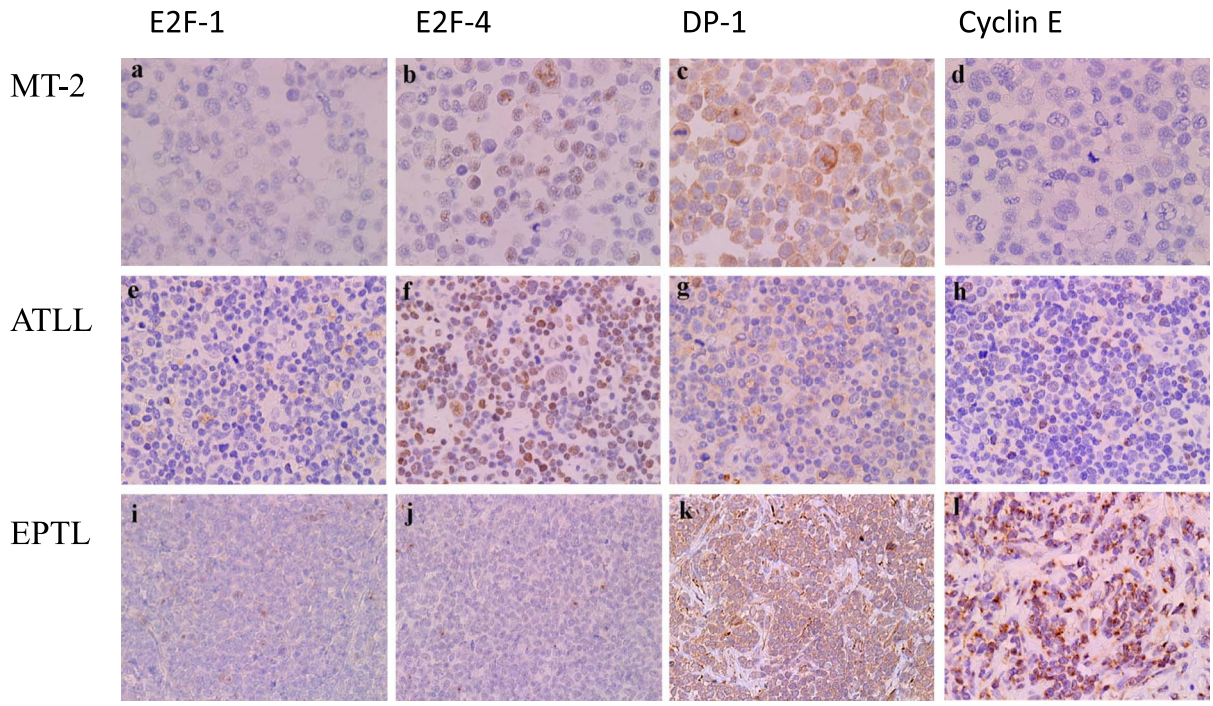

Fig. 12. G1 phase progression and G1–S phase transition detected by a panel of antibodies against E2F-1, E2F-4, DP-1, and cyclin E by the heating-AR and modified ImmunoMax/CSA method (DAB-H_2O_2 reaction and haematoxylin nuclear counterstaining, ×40 Olympus BX50, FUJIFILM HC-300). **a–d**) MT-2. **e–h**) ATLL. **i–l**) Peripheral T-cell lymphoma in Europeans (EPTL). **a, e**, and **i**) E2F-1. **b, f**, and **j**) E2F-4. **c, g**, and **k**) DP-1. **d, h**, and **l**) Cyclin E. The expression pattern of E2F-1 and E2F-4 is different between ATLL and EPTL. The expression pattern of cyclin E is also different between ATLL and EPTL.

transition may be damaged or neoplastic in ATLL, where the obscure co-expression of E2F-1 and E2F-4 observed in EPTL was thought to be their physiological expression. The mechanism of HBZ mRNA activating E2F-1 to propel the G1–S phase transition in the cell cycle of ATLL cells [23, 64, 65] was not identified by the heating AR and modified ImmunoMax/CSA method, although the method could visualize physiological expression of E2F-1, E2F-4, DP-1, and cyclin E. Further studies are necessary to elucidate the pathogenicity of HBZ mRNA and protein in ATLL.

Enzymatic-AR and nsCSA system of Lt-4 demonstrated obvious granular staining in a smaller number of ATLL cells than expected, as mentioned above, suggesting that the undigested, probable complex present form of Tax may be a feature of young ATLL cells derived from ATLL stem cells [51]. Since the "stemness" of stem cells allows their original features to be maintained, the dependency of early ATLL cells on Tax would be a feature of ATLL stem cells. Heating-AR and nsCSA system of CD117 [50] (Table 3) might be one way of investigating ATLL stem cells. Further studies are warranted to clarify the features of ATLL stem cells.

V. The Future Prospects of Ultra-IHC

In light of the fact that ultra-IHC has now been established. We introduce ultra-IHC into the field of human archival pathology specimens. Recently, the intercalated antibody-enhanced polymer (IAEP) method comprising the primary mouse monoclonal antibody reaction, secondary anti-mouse Ig rabbit polyclonal antibody, and anti-mouse anti-rabbit Ig- and HRP-labeled polymer reagent reaction, succeeded in detecting the over-expression of ALK-fusion protein that could not labeled by ordinary-IHC [98]. However, it appears that the physiological expression of some antigens is not detected by ordinary-IHC and IAEP methods. Ultra-IHC could label the physiological expression of the tumor-suppressor gene product, p53 protein, and cell cycle-related molecules: E2F-1, E2F-4, DP-1, and cyclin E. We demonstrated through ultra-IHC that the staining of its physiological expression was different from that of inactivated/phosphorylated p53 protein. We also demonstrated the physiological expression patterns of E2F-1, E2F-4, DP-1, and cyclin E in EPTL and their neoplastic and altered expression patterns in ATLL. Therefore, ultra-IHC has the capability to bring IHC of human archival pathology specimens to the next level, where the physiological expression and inactivation of several kinds of molecules can be detected.

The pathogenicity of HTLV-1 was that of Tax, although it is often stated that Tax is not expressed in ATLL. This review reported that ultra-IHC could detect minute amount of simple and complex present forms of Tax in ATLL cells, suggesting that Tax is expressed in ATLL cells. We must keep in mind that extremely small amounts of Tax could be detected by ultra-IHC in most cases of ATLL that is reported to indicate Tax-induced modes of signal transductions. Since atypical lymphocytes in HANNLA and ATLL cells express much less Tax than MT-2 cells [30], as mentioned above and shown in Figure 3, the Tax-induced molecular events listed in Table 2 have to be re-evaluated in the cases of high and low Tax expression in HTLV-1 infected cells probably under constant expression of HBZ mRNA and protein. The molecular events induced by low Tax expression may play roles in ATLL oncogenesis, which spans more than 30 years under anti-HTLV-1 immunity.

In the field of hematopathology, PBTS is a powerful archival pathology specimen, in which PBMCs can be examined through histochemistry including ultra-IHC. Ultra-IHC on PBTS is expected to enable monitoring of various changes in PBMCs in ATLL oncogenesis.

VI. Acknowledgments

The authors thank Prof. Alfred C Feller and Prof. Hartmut Merz (Institute of Pathology, University of Lübeck, Germany) for giving Kazuhisa Hasui the opportunity to learn the ImmunoMax method at their laboratory in 1995, and Emeritus Prof. Eiichi Sato and Emeritus Prof. Fusayoshi Murata (Kagoshima University) for their scientific assistance in developing the modified ImmunoMax method and new simplified CSA system. The authors also thank Prof. Mitsuru Setoyama (Department of Dermatology, Miyazaki University), Dr. Shuichi Hanada (Department of Hematology, Kagoshima Medical Center), Director Dr. Atae Utsunomiya (Department of Hematology, Imamura-Bunin Hospital), Prof. Martin-Leo Hansmann (Department of Pathology, University of Frankfurt (Johann Wolfgang Goethe-Universität Frankfurt am Main)) and Dr. Yukie Tashiro (Department of Pathology, Imakiire General Hospital) for granting us permission to investigate pathology specimens of ATLL and related diseases and Prof. Suguru Yonezawa (Department of Human Pathology, Kagoshima University) for processing peripheral blood tissue specimens.

This study was supported by Grants-in-Aid for Scientific Research C10670166 (Hasui K) and B13557017 (Hasui K), and the Japan Science and Technology Agency (JST) Innovation Satellite of Miyazaki FS (2006, Hasui K).

VII. References

1. Adya, N. and Giam, C. Z. (1995) Distinct regions in human T-cell lymphotropic virus type 1 tax mediate interactions with activator protein CREB and basal transcription factors. *J. Virol.* 69; 1834–1841.
2. Akagi, T., Ono, H. and Shimotohno, K. (1996) Expression of cell-cycle regulatory genes in HTLV-I infected T-cell lines: possible involvement of Tax1 in the altered expression of cyclin D2, p18Ink4 and p21Waf1/Cip1/Sdi1. *Oncogene* 12; 1645–1652.
3. Akagi, T. and Shimotohno, K. (1993) Proliferative response of Tax1-transduced primary human T cells to anti-CD3 antibody stimulation by an interleukin-2-independent pathway. *J. Virol.* 67; 1211–1217.
4. Arisawa, K., Soda, M., Endo, S., Kurokawa, K., Katamine, S.,

Shimokawa, I., Koba, T., Takahashi, T., Saito, H., Doi, H. and Shirahama, S. (2000) Evaluation of adult T-cell leukemia/lymphoma incidence and its impact on non-Hodgkin lymphoma incidence in southwestern Japan. *Int. J. Cancer* 85; 319–324.

5. Ariumi, Y., Kaida, A., Lin, J. Y., Hirota, M., Masui, O., Yamaoka, S., Taya, Y. and Shimotohno, K. (2000) HTLV-1 tax oncoprotein represses the p53-mediated trans-activation function through coactivator CBP sequestration. *Oncogene* 19; 1491–1499.
6. Arnulf, B., Villemain, A., Nicot, C., Mordelet, E., Charneau, P., Kersual, J., Zermati, Y., Mauviel, A., Bazarbachi, A. and Hermine, O. (2002) Human T-cell lymphotropic virus oncoprotein Tax represses TGF-beta 1 signaling in human T cells via c-jun activation: a potential mechanism of HTLV-1 leukemogenesis. *Blood* 100; 4129–4138.
7. Azimi, N., Brown, K., Bamford, R. N., Tagaya, Y., Siebenlist, U. and Waldmann, T. A. (1998) Human T cell lymphotropic virus type 1 Tax protein trans-activates interleukin15 gene transcription through an NF-kappaB site. *Proc. Natl. Acad. Sci. U S A* 95; 2452–2457.
8. Azimi, N., Jacobson, S., Leist, T. and Waldmann, T. A. (1999) Involvement of IL-15 in the pathogenesis of human T lymphotropic virus type 1-associated myelopathy/tropical spastic paraparesis: implications for therapy with a monoclonal antibody directed to the IL-2/15R beta receptor. *J. Immunol.* 163; 4064–4072.
9. Ballard, D. W., Bohnlein, E., Lowenthal, J. W., Wano, Y., Franza, B. R. and Greene, W. C. (1988) HTLV-1 tax induces cellular proteins that activate the kappa B element in the IL-2 receptor alpha gene. *Science* 241; 1652–1655.
10. Baranger, A. M., Palmer, C. R., Hamm, M. K., Giebler, H. A., Brauweiler, A., Nyborg, J. K. and Schepartz, A. (1995) Mechanism of DNA-binding enhancement by the human T-cell leukaemia virus transactivator Tax. *Nature* 376; 606–608.
11. Bex, F. and Gaynor, R. (1998) Regulation of gene expression by HTLV-1 Tax protein. *Methods* 16; 83–94.
12. Caron, C., Rousset, R., Beraud, C., Moncollin, V., Egly, J. M. and Jalinot, P. (1993) Functional and biochemical interaction of the HTLV-1 Tax1 transactivator with TBP. *EMBO J.* 12; 4269–4278.
13. Che, X. F., Zheng, C. L., Owatari, S., Mutoh, M., Gotanda, T., Jeung, H. C., Furukawa, T., Ikeda, R., Yamamoto, M., Haraguchi, M., Arima, N. and Akiyama, S. (2006) Overexpression of survivin in primary ATL cells and sodium arsenite induces apoptosis by down-regulating survivin expression in ATL cell lines. *Blood* 107; 4880–4887.
14. Ching, Y. P., Chun, A. C., Chin, K. T., Zhang, Z. Q., Jeang, K. T. and Jin, D. Y. (2004) Specific TATAA and bZIP requirements suggest that HTLV-1 Tax has transcriptional activity subsequent to the assembly of an initiation complex. *Retrovirology* 1; 18.
15. Chu, Z. L., Shin, Y. A., Yang, J. M., DiDonato, J. A. and Ballard, D. W. (1999) IKKgamma mediates the interaction of cellular IkappaB kinases with the tax transforming protein of human T-cell leukemia virus type 1. *J. Biol. Chem.* 274; 15297–15300.
16. Chung, H. K., Young, H. A., Goon, P. K., Heidecker, G., Princler, G. L., Shimozato, O., Taylor, G. P., Bangham, C. R. and Derse, D. (2003) Activation of interleukin-13 expression in T-cells from HTLV-1-infected individuals and in chronically infected cell lines. *Blood* 102; 4130–4136.
17. Costa, P. P., Jacobsson, B., Collins, V. P. and Biberfeld, P. (1986) Unmasking antigen determinants in amyloid. *J. Histochem. Cytochem.* 34; 1683–1685.
18. Ego, T., Tanaka, Y. and Shimotohno, K. (2005) Interaction of HTLV-1 Tax and methyl-CpG-binding domain 2 positively regulates the gene expression from the hypermethylated LTR. *Oncogene* 24; 1914–1923.
19. Fan, J., Ma, G., Nosaka, K., Tanabe, J., Satou, Y., Koito, A., Wain-Hobson, S., Vartanian, J. P. and Matsuoka, M. (2010) APOBEC3G generates nonsense mutations in human T-cell leukemia virus type 1 proviral genomes in vivo. *J. Virol.* 84; 7278–7287.
20. Fung, M. M., Chu, Y. L., Fink, J. L., Wallace, A. and McGuire, K. L. (2005) IL-2- and STAT5-regulated cytokine gene expression in cells expressing the Tax protein of HTLV-1. *Oncogene* 24; 4624–4633.
21. Gabet, A. S., Mortreux, F., Charneau, P., Riou, P., Duc-Dodon, M., Wu, Y., Jeang, K. T. and Wattel, E. (2003) Inactivation of hTERT transcription by Tax. *Oncogene* 22; 3734–3741.
22. Good, L., Maggirwar, S. B. and Sun, S. C. (1996) Activation of the IL-2 gene promoter by HTLV-1 tax involves induction of NK-AT complexes bound to the CD28-responsive element. *EMBO J.* 15; 3744–3750.
23. Grassmann, R., Aboud, M. and Jeang, K. T. (2005) Molecular mechanisms of cellular transformation by HTLV-1 Tax. *Oncogene* 24; 5976–5985.
24. Haller, K., Ruckes, T., Schmitt, I., Saul, D., Derow, E. and Grassmann, R. (2000) Tax-dependent stimulation of G1 phase-specific cyclindependent kinases and increased expression of signal transduction genes characterize HTLV type 1-transformed T cells. *AIDS Res. Hum. Retroviruses* 16; 1683–1688.
25. Haller, K., Wu, Y., Derow, E., Schmitt, I., Jeang, K. T. and Grassmann, R. (2002) Physical interaction of human T-cell leukemia virus type 1 Tax with cyclin-dependent kinase 4 stimulates the phosphorylation of retinoblastoma protein. *Mol. Cell. Biol.* 22; 3327–3338.
26. Harhaj, E. W. and Sun, S. C. (1999) IKKgamma serves as a docking subunit of the IkappaB kinase (IKK) and mediates interaction of IKK with the human T-cell leukemia virus Tax protein. *J. Biol. Chem.* 274; 22911–22914.
27. Hasui, K., Jia, H. M., Jia, X. S., Nomoto, M. and Sato, E. (1995) Antigen retrieval in paraffin-immunohistochemistry detecting monoclonality of immunoglobulin light chain in B-cell malignant lymphomas. In "Lymphoreticular Cells and Disease, Proceedings of the Fourth Japanese-Korean Lymphoreticular Workshop", ed. by H. Hara and J. D. Lee, Lymphoreticular Study Group, Department of Pathology, Kochi Medical School, Nankoku, Japan, pp. 321–329.
28. Hasui, K. and Murata, F. (2005) A new simplified catalyzed signal amplification system for minimizing non-specific staining in tissues with supersensitive immunohistochemistry. *Arch. Histol. Cytol.* 68; 1–17.
29. Hasui, K., Sato, E., Higashi, M., Horinouchi, M., Hanada, S., Yashiki, S., Izumo, S., Sonoda, S. and Osame, M. (1999) Expression of E2F transcription factors in adult T-cell leukemia/lymphoma cells in vivo; a highly sensitive immunohistochemical study. In "Lymphoreticular Cells and Diseases. Proceedings of the Sixth Japanese-Korean Lymphoreticular Workshop" ed. by T. Akagi and H. J. Ree, Lymphoreticular Study Group, Department of Pathology, Okayama University Medical School, Okayama, Japan, pp. 89–101.
30. Hasui, K., Sato, E., Tanaka, Y., Yashiki, S. and Izumo, S. (1997) Quantitative highly-sensitive immunohistochemistry (Modified ImmunoMax) of HTLV-1 p40tax and p27rex proteins in HTLV-1-associated non-neoplastic lymphadenopathy (HANNLA) with estimation of HTLV-1 dose by polymerase chain reaction. *DENDRITIC CELLS* 7; 19–27.
31. Hasui, K., Sato, E., Tanaka, Y., Yashiki, S. and Izumo, S. (1997) The modified ImmunoMax of HTLV-1 tax protein can label HTLV-1-related cases in T-cell lymphomas. In "Lymphoreticular Cells and Diseases. Proceedings of the Fifth Korean-Japanese Lymphoreticular Workshop" ed. by J. D. Lee and K. Takahashi, Hemato-lymphoreticular Study Group, The Korean

Society of Pathologists, Seoul, pp. 326–336.
32. Hasui, K., Shirahama, H., Sueyoshi, K., Sato, E. and Imakuma, M. (1996) Metachronous occurrence of gastric T-cell rich B-cell lymphoma and nodal T-cell lymphoma in a HTLV-1 carrier. *DENDRITIC CELLS* 6; 14–21.
33. Hasui, K., Sueyoshi, K., Kitajima, S. and Sato, E. (1992) HTLV-1-associated non-neoplastic lymphoadenopathy: Atypical follicular lesions of lymph nodes found in anti-human T-cell leukemia virus type 1 (HTLV-1) antibodies-positive subjects without neoplastic disorders. In "Lymphoreticular Cells, Fundamentals and Pathology, Proceedings of the Second Japanese-Korean Lymphoreticular Workshop" ed. by K. Takahashi and S. H. Kim, Lymphoreticular Cell Foundation, Kumamoto, pp. 239–251.
34. Hasui, K., Takatsuka, T., Sakamoto, R., Su, L., Matsushita, S., Tsuyama, S., Izumo, S. and Murata, F. (2002) Improvement of supersensitive immunohistochemistry with an autostainer: a simplified catalyzed signal amplification system. *Histochem. J.* 34; 215–222.
35. Hasui, K., Utsunomiya, A., Izumo, S., Goto, M., Yonezawa, S., Sato, E., Kanzaki, T. and Murata, F. (2003) An immunohistochemical analysis of peripheral blood tissue specimens from leukemia cells: Leukemic cells of adult T-cell leukemia/lymphoma express p40Tax protein of human T-cell lymphotropic virus type 1 when entering reproliferation. *Acta Histochem. Cytochem.* 36; 345–352.
36. Hinuma, Y., Nagata, K., Hanaoka, M., Nakai, M., Matsumoto, T., Kinoshita, K. I., Shirakawa, S. and Miyoshi, I. (1981) Adult T-cell leukemia: antigen in an ATL cell line and detection of antibodies to the antigen in human sera. *Proc. Natl. Acad. Sci. U S A* 78; 6476–6480.
37. Hirata, A., Higuchi, M., Niinuma, A., Ohashi, M., Fukushi, M., Oie, M., Akiyama, T., Tanaka, Y., Gejyo, F. and Fujii, M. (2004) PDZ domain-binding motif of human T-cell leukemia virus type 1 Tax oncoprotein augments the transforming activity in a rat fibroblast cell line. *Virology* 318; 327–336.
38. Hoyos, B., Ballard, D. W., Bohnlein, E., Siekevitz, M. and Greene, W. C. (1989) Kappa B-specific DNA binding proteins: role in the regulation of human interleukin-2 gene expression. *Science* 244; 457–460.
39. Huang, Y., Ohtani, K., Iwanaga, R., Matsumura, Y. and Nakamura, M. (2001) Direct trans-activation of the human cyclin D2 gene by the oncogene product Tax of human T-cell leukemia virus type I. *Oncogene* 20; 1094–1102.
40. Igakura, T., Stinchcombe, J. C., Goon, P. K. C., Taylor, G. P., Weber, J. N., Griffiths, G. M., Tanaka, Y., Osame, M. and Bangham, C. R. M. (2003) Spread of HTLV-I between lymphocytes by virus-induced polarization of the cytoskeleton. *Science* 299; 1713–1716.
41. Iha, H., Kibler, K. V., Yedavalli, V. R., Peloponese, J. M., Haller, K., Miyazato, A., Kasai, T. and Jeang, K. T. (2003) Segregation of NF-kappaB activation through NEMO/IKKgamma by Tax and TNFalpha: implications for stimulus-specific interruption of oncogenic signaling. *Oncogene* 22; 8912–8923.
42. Inoue, M., Matsuoka, M., Yamaguchi, K., Takatsuki, K. and Yoshida, M. (1998) Characterization of mRNA expression of IkappaB alpha and NF-kappaB subfamilies in primary adult T-cell leukemia cells. *Jpn. J. Cancer Res.* 89; 53–59.
43. Iwanaga, R., Ohtani, K., Hayashi, T. and Nakamura, M. (2001) Molecular mechanism of cell cycle progression induced by the oncogene product Tax of human T-cell leukemia virus type I. *Oncogene* 20; 2055–2067.
44. Iwanaga, Y., Kasai, T., Kibler, K. and Jeang, K. T. (2002) Characterization of regions in hsMAD1 needed for binding hsMAD2. A polymorphic change in an hsMAD1 leucine zipper affects MAD1-MAD2 interaction and spindle checkpoint function. *J. Biol. Chem.* 277; 31005–31013.
45. Jeang, K. T., Widen, S. G., Semmes, O. J. 4th and Wilson, S.H. (1990) HTLV-I trans-activator protein, tax, is a trans-repressor of the human beta-polymerase gene. *Science* 247; 1082–1084.
46. Jin, D. Y., Giordano, V., Kibler, K. V., Nakano, H. and Jeang, K. T. (1999) Role of adapter function in oncoprotein-mediated activation of NK-kappaB. Human T-cell leukemia virus type 1 Tax interact directly with IkappaB kinase gamma. *J. Biol. Chem.* 274; 17402–17405.
47. Jin, D. Y., Spencer, F. and Jeang, K. T. (1998) Human T cell leukemia virus type 1 oncoprotein Tax targets the human mitotic checkpoint protein MAD1. *Cell* 93; 81–91.
48. Jin, D. Y., Teramoto, H., Giam, C. Z., Chun, R. F., Gutkind, J. S. and Jeang, K. T. (1997) A human suppressor of c-Jun N-terminal kinase 1 activation by tumor necrosis factor alpha. *J. Biol. Chem.* 272; 25816–25823.
49. Kao, S. Y., Lemoine, F. J. and Marriott, S. J. (2001) p53-independent induction of apoptosis by the HTLV-I tax protein following UV irradiation. *Virology* 291; 292–298.
50. Kato, K., Hasui, K., Wang, J., Kawano, Y., Aikou, T. and Murata, F. (2008) Homeostatic mass control in gastric non-neoplastic epithelia under infection of Helicobacter pylori: An immunohistochemical analysis of cell growth, stem cells and programmed cell death. *Acta Histochem. Cytochem.* 41; 23–38.
51. Kayo, H., Yamazaki, H., Nishida, H., Dang, N. H. and Morimoto, C. (2007) Stem cell properties and the side population cells as a target for interferon-alpha in adult T-cell leukemia/lymphoma. *Biochem. Biophys. Res. Commun.* 364; 808–814.
52. Kehn, K., Fuente, C. L., Strouss, K., Berro, R., Jiang, H., Brady, J., Mahieux, R., Pumfery, A., Bottazzi, M. E. and Kashanchi, F. (2005) The HTLV-I Tax oncoprotein targets the retinoblastoma protein for proteasomal degradation. *Oncogene* 24; 525–540.
53. Kihler, K. V. and Jeang, K. T. (2001) CREB/ATF-dependent repression of cyclin A by human T-cell leukemia virus type 1 Tax protein. *J. Virol.* 75; 2161–2173.
54. Kim, S. J., Kehrl, J. H., Burton, J., Tendler, C. L., Jeang, K. T., Danielpour, D., Thevenin, C., Kim, K. Y., Sporn, M. B. and Roberts, A. B. (1990) Transactivation of the transforming growth factor beta 1 (TGF-beta 1) gene by human T lymphotropic virus type 1 tax: a potential mechanism for the increased production of TGF-beta 1 in adult T cell leukemia. *J. Exp. Med.* 172; 121–129.
55. Lee, B., Tanaka, Y. and Tozawa, H. (1989) Monoclonal antibody defining tax protein of human T-cell leukemia virus type-I. *Tohoku J. Exp. Med.* 157; 1–11.
56. Lee, D. K., Kim, B. C., Brady, J. N., Jeang, K. T. and Kim, S. J. (2002) Human T-cell lymphotropic virus type 1 tax inhibits transforming growth factor-beta signaling by blocking the association of Smad proteins with Smad-binding element. *J. Biol. Chem.* 277; 33766–33775.
57. Lemasson, I., Thebault, S., Sardet, C., Devaux, C. and Mesnard, J. M. (1998) Activation of E2F-mediated transcription by human Tcell leukemia virus type I Tax protein in a p16(INK4A)-negative T-cell line. *J. Biol. Chem.* 273; 23598–23604.
58. Li, J., Li, H. and Tsai, M. D. (2003) Direct binding of the N-terminus of HTLV-1 tax oncoprotein to cyclin-dependent kinase 4 is a dominant path to stimulate the kinase activity. *Biochemistry* 42; 6921–6928.
59. Liu, B., Hong, S., Tang, Z., Yu, H. and Giam, C. Z. (2005) HTLV-1 Tax directly binds the Cdc20-associated anaphase-promoting complex and activates it ahead of schedule. *Proc. Natl. Acad. Sci. U S A* 102; 63–68.
60. Liu, Y., Wang, Y., Yamakuchi, M., Masuda, S., Tokioka, T., Yamaoka, S., Maruyama, I. and Kitajima, I. (2001) Phosphoinositide-3 kinase-PKB/Akt pathway activation is involved in fibroblast Rat-1 transformation by human T-cell leukemia virus type I tax. *Oncogene* 20; 2514–2526.

61. Low, K. G., Dorner, L. F., Fernando, D. B., Grossman, J., Jeang, K. T. and Comb, M. J. (1997) Human T-cell leukemia virus type 1 Tax releases cell cycle arrest induced by p16INK4a. *J. Virol.* 71; 1956–1962.
62. Marin, O., Hasui, K., Remondegui, C., Sato, E., Aye, M. M., Takenouchi, N., Izumo, S. and Tajima, K. (2002) Adult T-cell leukemia/lymphoma in Jujuy, north-west Argentina. *Pathol. Int.* 52; 348–357.
63. Mariner, J. M., Lantz, V., Waldmann, T. A. and Azimi, N. (2001) Human T cell lymphotropic virus type 1 Tax activates IL-15R alpha gene expression through an NF-kappa B site. *J. Immunol.* 166; 2602–2609.
64. Matsuoka, M. and Jeang, K. T. (2007) Human T-cell leukaemia virus type 1 (HTLV-1) infectivity and cellular transformation. *Nat. Rev. Cancer* 7; 270–280.
65. Matsuoka, M. (2010) HTLV-1 bZIP factor gene: Its roles in HTLV-1 pathogenesis. *Mol. Aspects Med.* 31; 359–366.
66. McGuire, K. L., Curtiss, V. E., Larson, E. L. and Haseltine, W. A. (1993) Influence of human T-cell leukemia virus type 1 tax and rex on interleukin-2 gene expression. *J. Virol.* 67; 1590–1599.
67. Merz, H., Malisius, R., Mannweiler, S., Zhou, R., Hartmann, W., Orscheschek, K., Moubayed, P. and Feller, A. C. (1995) ImmunoMax. A maximized immunohistochemical method for the retrieval and enhancement of hidden antigens. *Lab. Invest.* 73; 149–156.
68. Migone, T. S., Lin, J. X., Cereseto, A., Mulloy, J. C., O'Shea, J. J., Franchini, G. and Leonard, W. J. (1995) Constitutively activated Jak-STAT pathway in T cells transformed with HTLV-1. *Science* 269; 79–81.
69. Moon, J. J., Rubio, E. D., Martino, A., Krumm, A. and Nelson, B. H. (2004) A permissive role for phosphatidylinositol 3-kinase in the Stat5-mediated expression of cyclin D2 by the interleukin-2 receptor. *J. Biol. Chem.* 279; 5520–5527.
70. Mulloy, J. C., Kislyakova, T., Cereseto, A., Casareto, L., LoMonico, A., Fullen, J., Lorenzi, M. V., Cara, A., Nicot, C., Giam, C. and Franchini, G. (1998) Human T-cell lymphotropic/leukemia virus type 1 Tax abrogates p53-induced cell cycle arrest and apoptosis through its CREB/ATF functional domain. *J. Virol.* 72; 8852–8860.
71. Nagura, H., Brandtzaeg, P., Nakane, P. K. and Brown, W. R. (1979) Ultrastructural localization of J chain in human intestinal mucosa. *J. Immunol.* 123; 1044–1050.
72. Neuveut, C. and Jeang, K. T. (2002) Cell cycle dysregulation by HTLV-I: role of the tax oncoprotein. *Front. Biosci.* 7; d157–d163.
73. Neuveut, C., Low, K. G., Maldarelli, F., Schmitt, I., Majone, F., Grassmann, R. and Jeang, K. T. (1998) Human T-cell leukemia virus type 1 Tax and cell cycle progression: role of cyclin D-cdk and p110Rb. *Mol. Cell Biol.* 18; 3620–3632.
74. Ohshima, K., Suzumiya, J., Kato, A., Tashiro, K. and Kikuchi, M. (1997) Clonal HTLV-I-infected CD4+ T-lymphocytes and non-clonal non-HTLV-I-infected giant cells in incipient ATLL with Hodgkin-like histologic features. *Int. J. Cancer* 72; 592–598.
75. Ohtani, K., Iwanaga, R., Arai, M., Huang, Y., Matsumura, Y. and Nakamura, M. (2000) Cell type-specific E2F activation and cell cycle progression induced by the oncogene product Tax of human T-cell leukemia virus type I. *J. Biol. Chem.* 275; 11154–11163.
76. Okamoto, T., Ohno, Y., Tsugane, S., Watanabe, S., Shimoyama, M., Tajima, K., Miwa, M. and Shimotohno, K. (1989) Multi-step carcinogenesis model for adult T-cell leukemia. *Jpn. J. Cancer Res.* 80; 191–195.
77. Okamura, J., Utsunomiya, A., Tanosaki, R., Uike, N., Sonoda, S., Kannagi, M., Tomonaga, M., Harada, M., Kimura, N., Masuda, M., Kawano, F., Yufu, Y., Hattori, H., Kikuchi, H. and Saburi, Y. (2005) Allogeneic stem-cell transplantation with reduced conditioning intensity as a novel immunotherapy and antiviral therapy for adult T-cell leukemia/lymphoma. *Blood* 105; 4143–4145.
78. Pankow, R., Durkop, H., Latza, U., Krause, H., Kunzendorf, U., Pohl, T. and Bulfone-Paus, S. (2000) The HTLV-1 tax protein transcriptionally modulates OX40 antigen expression. *J. Immunol.* 165; 263–270.
79. Park, H. U., Jeong, J. H., Chung, J. H. and Brady, J. N. (2004) Human T-cell leukemia virus type 1 Tax interacts with Chk1 and attenuates DNA-damage induced G2 arrest mediated by Chk1. *Oncogene* 23; 4966–4974.
80. Pise-Masison, C. A., Radonovich, M., Sakaguchi, K., Appella, E. and Brady, J. N. (1998) Phosphorylation of p53: a novel pathway for p53 inactivation in human T-cell lymphotropic virus type 1-transformed cells. *J. Virol.* 72; 6348–6355.
81. Ruben, S., Poteat, H., Tan, T. H., Kawakami, K., Roeder, R., Haseltine, W. and Rosen, C. A. (1988) Cellular transcription factors and regulation of IL-2 receptor gene expression by HTLV-1 tax gene product. *Science* 241; 89–92.
82. Saintigny, Y., Dumay, A., Lambert, S. and Lopez, B. S. (2001) A novel role for the Bcl-2 protein family: specific suppression of the RAD51 recombination pathway. *EMBO J.* 20; 2596–2607.
83. Santiago, F., Clark, E., Chong, S., Molina, C., Mozafari, F., Mahieux, R., Fujii, M., Azimi, N. and Kashanchi, F. (1999) Transcriptional up-regulation of the cyclin D2 gene and acquisition of new cyclin-dependent kinase partners in human T-cell leukemia virus type 1-infected cells. *J. Virol.* 73; 9917–9927.
84. Sasaki, H., Nishikata, I., Shiraga, T., Akamatsu, E., Fukami, T., Hidaka, T., Kubuki, Y., Okayama, A., Hamada, K., Okabe, H., Murakami, Y., Tsubouchi, H. and Morishita, K. (2005) Over-expression of a cell adhesion molecule, TSLC1, as a possible molecular marker for acute-type adult T-cell leukemia. *Blood* 105; 1204–1213.
85. Schmitt, I., Rosin, O., Rohwer, P., Gossen, M. and Grassmann, R. (1998) Stimulation of cyclin-dependent kinase activity and G1- to S-phase transition in human lymphocytes by the human T-cell leukemia/lymphotropic virus type 1 Tax protein. *J. Virol.* 72; 633–640.
86. Shi, S. R., Cote, R. J. and Taylor, C. R. (1997) Antigen retrieval immunohistochemistry: past, present, and future. *J. Histochem. Cytochem.* 45; 327–343.
87. Shi, S. R., Cote, R. J. and Taylor, C. R. (2001) Antigen retrieval techniques: current perspectives. *J. Histochem. Cytochem.* 49; 931–937.
88. Shi, S. R., Key, M. E. and Kalra, K. L. (1991) Antigen retrieval in formalin-fixed, paraffin-embedded tissues: an enhancement method for immunohistochemical staining based on microwave oven heating of tissue sections. *J. Histochem. Cytochem.* 39; 741–748.
89. Shimoyama, M. (1991) Diagnostic criteria and classification of clinical subtypes of adult T-cell leukemia/lymphoma. A report from the Lymphoma Study Group (1984–1987). *Br. J. Haematol.* 79; 428–437.
90. Sinha-Datta, U., Horikawa, I., Michishita, E., Datta, A., Sigler-Nicot, J. C., Brown, M., Kazanji, M., Barrett, J. C. and Nicot, C. (2004) Transcriptional activation of hTERT through the NF-kappaB pathway in HTLV-I-transformed cells. *Blood* 104; 2523–2531.
91. Siu, Y. T., Chin, K. T., Siu, K. L., Yee, W., Choy, E., Jeang, K. T. and Jin, D. Y. (2006) TORC1 and TORC2 coactivators are required for Tax activation of the human T-cell leukemia virus type 1 long terminal repeats. *J. Virol.* 80; 7052–7058.
92. Sonoda, J., Koriyama, C., Yamamoto, S., Kozako, T., Li, H. C., Lema, C., Yashiki, S., Fujiyoshi, T., Yoshinaga, M., Nagata, Y.,

Akiba, A., Takezaki, T., Yamada, K. and Sonoda, S. (2004) HTLV-1 provirus load in peripheral blood lymphocytes of HTLV-1 carriers is diminished by green tea drinking. *Cancer Sci.* 95; 596–601.

93. Suzuki, T., Kitao, S., Matsushime, H. and Yoshida, M. (1996) HTLV-1 Tax protein interacts with cyclin-dependent kinase inhibitor p16INK4A and counteracts its inhibitory activity towards CDK4. *EMBO J.* 15; 1607–1614.
94. Suzuki, T., Narita, T., Uchida-Toita, M. and Yoshida, M. (1999) Down-regulation of the INK4 family of cyclin-dependent kinase inhibitors by tax protein of HTLV-1 through two distinct mechanisms. *Virology* 259; 384–391.
95. Suzuki, T., Ohsugi, Y., Uchida-Toita, M., Akiyama, T. and Yoshida, M. (1999) Tax oncoprotein of HTLV-1 binds to the human homologue of Drosophila discs large tumor suppressor protein, hDLG, and perturbs its function in cell growth control. *Oncogene* 18; 5967–5972.
96. Takatsuki, K., Yaguchi, K., Watanabe, T., Mochizuki, M., Kiyokawa, T., Mori, S. and Miyata, N. (1992) Adult T-cell leukemia and HTLV-1 related diseases. In "Gann Monograph on Cancer Research No. 39. Advances in Adult T-cell Leukemia and HTLV-1 Research" ed. by K. Takatsuki, Y. Hinuma and M. Yoshida, Japan Scientific Societies Press, pp. 1–15.
97. Takenouchi, N., Matsuoka, E., Moritoyo, T., Nagai, M., Katsuta, K., Hasui, K., Ueno, K., Eizuru, Y., Usuku, K., Osame, M., Isashiki, Y. and Izumo, S. (1999) Molecular pathologic analysis of the tonsil in HTLV-I-infected individuals. *J. AIDS.* 22; 200–207.
98. Takeuchi, K., Choi, Y. L., Togashi, Y., Soda, M., Hatano, S., Inamura, K., Takada, S., Ueno, T., Yamashita, Y., Satoh, Y., Okumura, S., Nakagawa, K., Ishikawa, Y. and Mano, H. (2009) KIF5B-ALK, a novel fusion oncokinase identified by an immunohistochemistry-based diagnostic system for ALK-positive lung cancer. *Clin. Cancer Res.* 15; 3143–3149.
99. Tamiya, S., Matsuoka, M., Etoh, K., Watanabe, T., Kamihira, S., Yamaguchi, K. and Takatsuki, K. (1996) Two types of defective human T-lymphotropic virus type I provirus in adult T-cell leukemia. *Blood* 88; 3065–3073.
100. Tanaka, Y., Masuda, M., Yoshida, A., Shida, H., Nyunoya, H., Shimotohno, K. and Tozawa, H. (1992) An antigenic structure of the trans-activator protein encoded by human T-cell leukemia virus type-I (HTLV-I), as defined by a panel of monoclonal antibodies. *AIDS. Res. Hum. Retroviruses* 8; 227–235.
101. Tanimura, A., Dan, S. and Yoshida, M. (1998) Cloning of novel isoforms of the human Gli2 oncogene and their activities to enhance tax-dependent transcription of the human T-cell leukemia virus type 1 genome. *J. Virol.* 72; 3958–3964.
102. Van Orden, K., Yan, J. P., Ulloa, A. and Nyborg, J. K. (1999) Binding of the human T-cell leukemia virus Tax protein to the coactivator CBP interferes with CBP-mediated transcriptional control. *Oncogene* 18; 3766–3772.
103. Waeldele, K., Schneider, G., Ruckes, T. and Grassmann, R. (2004) Interleukin-13 overexpression by tax transactivation: a potential autocrine stimulus in human T-cell leukemia virus-infected lymphocytes. *J. Virol.* 78; 6081–6090.
104. Wang, J., Hasui, K., Jia, X. S., Matsuyama, T. and Eizuru, Y. (2009) Possible role for external environmental stimuli in nasopharyngeal NK/T-cell lymphomas in the northeast of China with EBV infection-related autophagic cell death: a pathoepidemiological analysis. *J. Clin. Exp. Hematop.* 49; 97–108.
105. Wang, J., Hasui, K., Utsunomiya, A., Jia, X. S., Matsuyama, T. and Murata, F. (2008) Association of high proliferation in adult T-cell leukemia cells with apoptosis and expression of p53 protein in acute type ATL. *J. Clin. Exp. Hematop.* 48; 1–10.
106. Watanabe, T. (2007) Molecular biology of HTLV-1. In "HTLV-1 and Diseases", ed. by T. Watanabe, S. Kamihira and K. Yamaguchi, BUNKOUDOU, pp. 166–177 (in Japanese).
107. Xu, X., Heidenreich, O., Kitajima, I., McGuire, K., Li, Q., Su, B. and Nerenberg, M. (1996) Constitutively activated JNK is associated with HTLV-1 mediated tumorigenesis. *Oncogene* 13; 135–142.
108. Yamada, Y. and Kamihira, S. (2008) Immunological aspects of adult T-cell leukemia/lymphoma (ATLL), a possible neoplasm of regulatory T-cells. *Current Immunology Reviews* 4; 242–250.
109. Yamaguchi, K., Seiki, M., Yoshida, M., Nishimura, H., Kawano, F. and Takatsuki, K. (1984) The detection of human T cell leukemia virus proviral DNA and its application for classification and diagnosis of T cell malignancy. *Blood* 63; 1235–1240.
110. Yoshida, M. and Fujisawa, J. (1992) Positive and negative regulation of HTLV-1 gene expression and their roles in leukemogenesis in ATLL. In "Gann Monograph on Cancer Research No. 39. Advances in Adult T-Cell Leukemia and HTLV-1 Research", ed. by K. Takatsuki, Y. Hinuma and M. Yoshida, Japan Scientific Societies Press, pp. 217–236.
111. Yoshida, M., Seiki, M., Yamaguchi, K. and Takatsuki, K. (1984) Monoclonal integration of human T-cell leukemia provirus in all primary tumors of adult T-cell leukemia suggests causative role of human T-cell leukemia virus in the disease. *Proc. Natl. Acad. Sci. U S A* 81; 2534–2537.
112. Yoshida, M. (2001) Multiple viral strategies of HTLV-1 for dysregulation of cell growth control. *Annu. Rev. Immunol.* 19; 475–496.